

We are IntechOpen, the world's leading publisher of Open Access books Built by scientists, for scientists

4,500

Open access books available

119,000

International authors and editors

135M

Downloads

Our authors are among the

154

Countries delivered to

TOP 1%

most cited scientists

12.2%

Contributors from top 500 universities



WEB OF SCIENCE™

Selection of our books indexed in the Book Citation Index
in Web of Science™ Core Collection (BKCI)

Interested in publishing with us?
Contact book.department@intechopen.com

Numbers displayed above are based on latest data collected.
For more information visit www.intechopen.com



Influence of Optical Phonons on Optical Transitions in Semiconductor Quantum Dots

Cheche Tiberius and Emil Barna
University of Bucharest/Faculty of Physics
Romania

1. Introduction

Accurate theoretical description of optical phenomena in semiconductor quantum dots (QDs) depends on the description accuracy of the energy structure of the QD. For the energy structure description the existent methods, such as, the tight-binding method, the effective bond-orbital model, the first-principles calculations or the multi-band approach within $\mathbf{k}\cdot\mathbf{p}$ theory, have some limitations either in the accuracy of the predicted electronic structures or the computation efficiency. In this context, the phonon influence on the optical properties makes the theoretical description of the optical phenomena in QDs more complex. In this chapter, we introduce several methods and techniques to describe the phonon influence on the emission and absorption spectra of semiconductor QDs. They are implemented on simplified models of QDs that can capture the main physics of the studied phenomena.

2. Phonons in optical transitions in nanocrystals. Theoretical background

The problem of the exciton-phonon interaction in zero-dimensional systems has a rich history. In principle, strong quantum confinement of the carriers or strong electron-phonon interaction induces increasing of the kinetic energy of the charge carriers involved in the optical transitions. In such cases, the optical transitions in nanocrystals are properly described by an *adiabatic* approach. On the other hand, if either the dynamic Jahn-Teller effect (in case the electronic levels are degenerate) or the pseudo-Jahn-Teller effect (in case the electronic inter-level energy is close to the optical phonon energy) is present, the electron-phonon system of the nanocrystal is properly described by a *non-adiabatic* approach. In this section, basic information regarding the optical transitions involving LO phonons, adapted to nano-crystals, is briefly introduced.

2.1 Adiabatic and non-adiabatic treatments of the optical transitions

Chemical compounds or solids, small or large molecules may be represented by an ensemble of interacting electrons and nuclei. Such complex systems are usually described by the Born-Oppenheimer approximation (Born & Oppenheimer, 1927), which separates the electronic and nuclear motions. This separation is made within the adiabatic approach, which means the electrons are much lighter and faster moving than the nuclei so they can

follow the nuclei around and can adjust practically instantaneously their positions. The Hamiltonian of the global system is

$$H(r, Q) = T_Q + T_r + U(r, Q) + V(Q) \equiv T_Q + H(r, Q) \quad (1)$$

where r, Q are the set of the generalised coordinates of electrons and nuclei, respectively, and $H(r, Q)$ is the *electronic Hamiltonian*. $U(r, Q)$ represents the electron-electron plus the electron-nucleus interactions and $V(Q)$ represents nucleus-nucleus interactions. The kinetic energy operators are $T_r = -\sum_n \hbar^2 (2m)^{-1} \partial^2 / \partial r_n^2$, $T_Q = -\sum_\alpha \hbar^2 (2M_\alpha)^{-1} \partial^2 / \partial Q_\alpha^2$, where n and α are indices of individual electronic and nuclear coordinates, respectively; m and M_α are the electronic mass and mass of the α -th nucleus, respectively.

Next, following (Newton & Sutin, 1984), we introduce the *diabatic* and *adiabatic* description of the electronic system by expanding the vibronic wave functions $\psi(r, Q)$ in the basis set of the orthonormal electronic wave functions, $\{\Phi_n(r, Q)\}$, by $\psi(r, Q) = \sum_n \Phi_n(r, Q) \xi_n(Q)$, where $\xi_n(Q)$ are Q -dependent parameters. The orthonormal electronic wavefunctions are found by solving the electronic Schrödinger equation in the Born-Oppenheimer approximation taking Q as a parameter

$$H(r, Q) \Phi(r, Q) = E(Q) \Phi(r, Q). \quad (2)$$

The solution $E_n(Q)$ of Eq. (2) corresponding to certain electronic wave function $\Phi_n(r, Q)$ are the so-called potential energy surfaces (PES). The expansion coefficients ξ can be found by solving the vibronic Schrödinger equation $H(r, Q) \psi(r, Q) = E \psi(r, Q)$, which leads to

$$\left[T_Q + (T_Q'')_{mn} + H_{mn}(Q) - E \right] \xi_{m\alpha}(Q) = - \sum_{n \neq m} \left[H_{mn}(Q) + (T_Q')_{mn} + (T_Q'')_{mn} \right] \xi_{n\alpha}(Q). \quad (3)$$

In Eq. (3) ξ acquires a new index α which quantifies the nuclear states. The matrix elements are defined as $(T_Q'')_{mn} = \langle m | T_Q | n \rangle$, and $(T_Q')_{mn} = -\sum_k \hbar^2 (M_k)^{-1} \langle m | \partial / \partial Q_k | n \rangle \partial / \partial Q_k$ (Dirac notation is used). In Eq. (3) we can write

$$(T_Q')_{mn} + (T_Q'')_{mn} = - \int dq \Phi_m^* \sum_k \frac{\hbar^2}{2M_k} \left[\frac{\partial^2 \Phi_n}{\partial Q_k^2} + 2 \left(\frac{\partial \Phi_n}{\partial Q_k} \right) \frac{\partial}{\partial Q_k} \right] = L_{mn}$$

where the operator

$$L = - \sum_k \frac{\hbar^2}{2M_k} \left[\frac{\partial^2 \Phi_n}{\partial Q_k^2} + 2 \left(\frac{\partial \Phi_n}{\partial Q_k} \right) \frac{\partial}{\partial Q_k} \right] \quad (4)$$

is the so-called Born-Oppenheimer breakdown (nuclear coupling) or non-adiabaticity operator. $H_{mn}(Q)$ from Eq. (3) is usually called electronic coupling term. In what follows for the clarity, we restrain discussion to only two electronic states. In studying the electron transition starting with Eq. (3) one frequently uses two basis sets:

- i. The diabatic (non-stationary or localised) basis containing $\{\Phi_i, \Phi_f\}$ (see Fig. 1). They are chosen as set of eigenfunctions of the suitable zeroth-order electronic Hamiltonian, H , where the interaction between the two electronic states Φ_i and Φ_f is removed. The corresponding PESs are $H_{ii}(Q) = \langle i | H | i \rangle$ and $H_{ff}(Q) = \langle f | H | f \rangle$.
- ii. The adiabatic (stationary or delocalised) basis containing $\{\Phi_1, \Phi_2\}$ (see Fig. 1). The corresponding PES are the *non-crossing* electronic terms, $H_{11}(Q) = \langle 1 | H | 1 \rangle$ and $H_{22}(Q) = \langle 2 | H | 2 \rangle$, and $H_{mm} = \left[(H_{ii} + H_{ff}) \pm \left[(H_{ii} - H_{ff})^2 + 4|H_{if}|^2 \right]^{\frac{1}{2}} \right] / 2$ with $m = 1, 2$ is relation between the eigenvalues of the two basis sets. The smallest energy difference between the two non-intersecting adiabatic PESs is $2H_{if}$. Transitions are classified as being adiabatic or non-adiabatic as function of the magnitude of the coupling matrix elements. The process is adiabatic if the matrix elements of T'_Q, T''_Q can be safely neglected, irrespective of basis used, either diabatic or adiabatic; if the adiabatic basis is chosen transition does not involve a tunneling between the two adiabatic states (surfaces). On the other hand, a reaction is non-adiabatic if there is no basis that permits the neglect of $(T'_Q)_{12}, (T''_Q)_{12}$; when the adiabatic basis is chosen transition involves a tunneling between the two adiabatic states (surfaces).

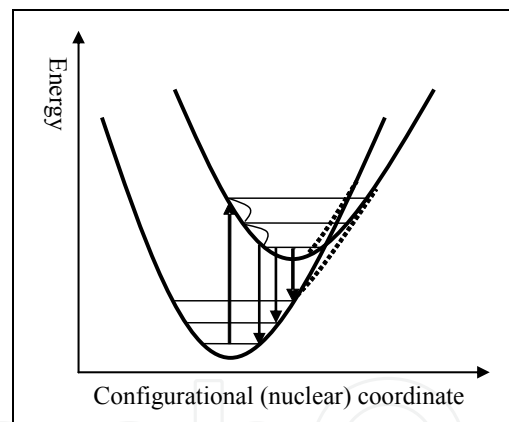


Fig. 1. Radiative adiabatic process in the diabatic/adiabatic picture.

Optical transitions can be produced by *tunnelling* or by *overcoming* the potential barrier. The PESs as function of a representative nuclear coordinate and the vibrational levels are sketched in Fig. 1 for the absorption/emission process by an adiabatic process. The vibrational levels represent the energy of longitudinal optical (LO) phonons, that have a fast relaxation. In this case, the possible tunneling induced by the nuclear coupling terms T' and T'' between the two adiabatic PESs has low probability, and the transition is radiative. The adiabatic PESs are drawn as non-intersecting PESs by the dotted line near the crossing point of the diabatic PESs (solid line). After photon absorption the nuclei in the material adjust position to their new equilibrium positions. The time of adjustment of order 10^{13} s is much faster than the spontaneous emission time of order 10^8 s and the system relaxes to the lowest vibrational level of the excited state. Then radiative transitions to the vibrational states of the

ground state are followed by subsequent relaxations to the lowest vibrational ground state. The mechanism explains the presence of LO phonon satellites in the photoluminescence (PL) spectra. In this scenario, one considers the transition from adiabatic upper PES to the lower adiabatic PES that is triggered by the nuclear coupling is of low probability. This low influence of the nuclear coupling on the process gives the adiabatic character of the transition. Otherwise, tunneling to the lowest adiabatic PES, which means a non-adiabatic process, followed by a non-radiative relaxation by multi-phonon emission is possible.

2.2 The Huang-Rhys factor

The Huang-Rhys factor is frequently used as roughly being a measure of the strength of the exciton-phonon coupling (Banyai & Koch, 1993; Woggon, 1997).

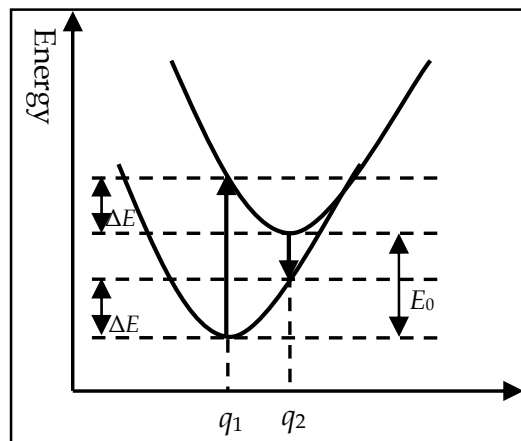


Fig. 2. PESs with the same force constant.

In a simple way, Huang-Rhys factor is introduced by using the configuration coordinate diagram, as sketched in Fig. 2. The PESs, E_g, E_e for the ground and excited states can be written for the model of a single frequency, ω , of the oscillators as $E_g = E_1 + \hbar\omega(q - q_1)^2/2$ and $E_e = E_2 + \hbar\omega(q - q_2)^2/2$, where q_1, q_2 are the equilibrium dimensionless coordinates. According to Fig. 2, we have

$$\Delta E = E_e(q_1) - E_2 = E_g(q_2) - E_1 = \frac{\hbar\omega}{2}(q_1 - q_2)^2 = g\hbar\omega, \quad (5)$$

and

$$\hbar\omega_{em} - \hbar\omega_{abs} = E_e(q_1) - E_g(q_1) - E_e(q_2) + E_g(q_2) = 2g\hbar\omega, \quad (6)$$

where g is the Huang-Rhys factor. In experiment, the energy difference between the maximum absorption peak and the emission peak is usually referred to as the Stokes shift. Eq. (6) is an approximate definition of the Stokes shift as well as of relation between the Stokes shift and the Huang-Rhys factor g (Ridley, 1988). Large values of g means a larger value between the minima of two PESs, $q_1 - q_2$.

Next, to make connection with the Hamiltonian of QD, we consider a system with the ground state $|g\rangle$, and two excited states $|i\rangle, |f\rangle$ in the diabatic representation. In this picture, the total Hamiltonian reads

$$H = |g\rangle H_g \langle g| + |i\rangle H_i \langle i| + |f\rangle H_f \langle f| + H_{if} (|i\rangle \langle f| + |f\rangle \langle i|) \quad (7)$$

where H_g is the ground state, H_i and H_f are the excited states, and H_{if} is the interaction between the excited states Hamiltonians. We consider for simplicity a single nuclear coordinate, the nuclear displacement relative to the equilibrium position, Q , with origin at the minimum of the ground state, and a single frequency of vibration of the phonon, ω . Assuming H_i , H_f , and H_{if} are linear dependent of Q , and a parabolic shape of the potential energy surfaces (PESs), we write $H_l = \varepsilon_l + P^2(2m)^{-1} + m\omega^2(Q + Q_l)^2/2$ (with $l = i, f$), $H_g = P^2(2m)^{-1} + m\omega^2 Q^2/2$, $H_{if} = \sqrt{2}(m\omega/\hbar)^{-1/2} C_{if} Q$, where ε_l is the zeroth-order energy separation between the l -th excited PES and the ground state PES, and C_{if} is a constant. Note that H_{if} is written in non-Condon approximation, that is, the nuclear coupling between the two excited states is Q dependent. Next, we introduce the dimensionless momentum $p = (\hbar m \omega)^{-1/2} P$, and dimensionless coordinate $q = (m\omega/\hbar)^{1/2} Q$, and obtain $H_g = \frac{\hbar\omega}{2}(p^2 + q^2)$, $H_i = \varepsilon_i + \frac{\hbar\omega}{2}[p^2 + (q + q_i)^2]$, $H_f = \varepsilon_f + \frac{\hbar\omega}{2}[p^2 + (q + q_f)^2]$, $H_{if} = \sqrt{2}C_{if}q$. Further progress is achieved by making the replacement $q = (a + a^+)/\sqrt{2}$, and $p = -i(a - a^+)/\sqrt{2}$, where a (a^+) are the usual annihilation (creation) boson operators. Thus, one obtains $H_g = \hbar\omega(a^+ a + 1/2)$, $H_{if} = C_{if}(a^+ + a)$, $H_i = \varepsilon_i + \hbar\omega[(a^+ a + 1/2) + (a^+ + a)q_i/\sqrt{2} + q_i^2]$, $H_f = \varepsilon_f + \hbar\omega[(a^+ a + 1/2) + (a^+ + a)q_f/\sqrt{2} + q_f^2]$.

With the closure relation $|g\rangle \langle g| + |i\rangle \langle i| + |f\rangle \langle f| = \mathbf{1}$ one obtains

$$H = \hbar\omega a^+ a + |i\rangle \varepsilon_i \langle i| + |f\rangle \varepsilon_f \langle f| + (M_i |i\rangle \langle i| + M_f |f\rangle \langle f|)(a^+ + a) + C_{if} (|i\rangle \langle f| + |f\rangle \langle i|)(a^+ + a) \quad (8)$$

where $\varepsilon_i' = \varepsilon_i + \hbar\omega(q_i^2 + 1)/2$, and $M_i = \hbar\omega q_i/\sqrt{2} = \hbar\omega\sqrt{g_i}$ in which g_i is the Huang-Rhys factor of the state $|i\rangle$ (similarly for the $|f\rangle$ state). In this single frequency model there is a simple dependence between the nuclear coupling and the Huang-Rhys factor, namely $M_i = \hbar\omega\sqrt{g_i}$. With introduction of the creation annihilation operators of electronic states by $|i\rangle \langle i| = C_i^+ C_i$ and $|i\rangle \langle f| = C_i^+ C_f$ (similarly for the $|f\rangle$ state), justified by $C_i^+ C_i |i\rangle = C_i^+ |g\rangle = |i\rangle$, $C_i^+ C_f |f\rangle = C_i^+ |g\rangle = |i\rangle = |i\rangle \langle f| f\rangle$, and $C_i^+ C_f |i\rangle = 0 = |i\rangle \langle f| i\rangle$, Eq. (8) reads

$$H = \hbar\omega a^+ a + \sum_{j=i,f} C_j^+ C_j [\varepsilon_j' + M_j (a^+ + a)] + C_{if} (C_i^+ C_f + C_f^+ C_i)(a^+ + a) \quad (9)$$

Eq. (9) describes interaction between an electronic system and phonons. It is of the form of the localized defect with several electronic states model, in the case the electronic states are

mixed by phonons. The discrete structure of levels in this model is appropriate for description of the 'atomic' energy structure of QDs, and this Hamiltonian is often adopted in QDs problems. Regarding the type of approach, an adiabatic treatment of QD implies absence in the Hamiltonian of the nuclear coupling between PESs, that is $C_{ij}=0$ or equivalently a non-mixing of the electronic states by phonons.

2.3 Absorption and emission spectra in nanocrystals

Often in experiment the Huang-Rhys factor for the LO phonons is calculated from the optical spectra as the ratio of 1LO and 0LO intensity lines, $I(1)/I(0)$. Justification is found within the adiabatic model of a localized impurity interacting with a set of mono-energetic phonons of frequency ω_0 (Einstein model, (Mahan, 2000)). Optical absorption spectrum is derived by evaluating the imaginary part of the one particle Green's function. One obtains that in limit of low temperatures the intensity ratio for the 1LO and 0LO spectral lines gives the Huang-Rhys factor, $g = \sum_{\mathbf{q}} M_{\mathbf{q}}^2 / (\hbar^2 \omega_0^2)$, with $M_{\mathbf{q}}$ the electron phonon coupling matrix element of the \mathbf{q} mode phonon. At $T=0$ the phonon replicas follow a Poisson distribution, $I(n) \propto g^n e^{-g} / n!$, in which n is the number of phonons generated in the transition and $g = I(1)/I(0)$. Thus, calculation of the Huang Rhys factor from the optical spectra as the ratio $I(1)/I(0)$ should be cautiously considered as far as it is valid in the limit of an adiabatic approach that assumes absence of mixing of the electronic levels by phonons.

3. Longitudinal optical phonons in optical spectra of defect-free semiconductor quantum dots

The presence of the strong phonon replicas in PL spectra of QDs of weakly polar III-V compounds is a striking result since no such strong phonon replicas are usually observed in the luminescence of III-V compounds, and not always in the PL spectra of QDs of other semiconductor types. The exciton-phonon coupling is already accepted as being strongly enhanced in semiconductor QDs, see, e.g., (Fomin et. al., 1998; Verzelen et. al., 2002; Cheche & Chang, 2005), but there are few theoretical reports (Peter et. al., 2004; Axt et. al., 2005) on the optical spectra of multiexciton complexes which take into account the phonon coupling. For spherical QDs the one-band models by which conduction and valence states are computed from single-particle Schrödinger equations in the effective mass approximation are a good approximation for type I heterostructures (Sercel & Vahala, 1990). In what follows, in Section 3.1 two models built starting with such one-band single-particle states are introduced for spherical and cylindrical shapes of QDs. A short discussion about LO phonon confinement completes this section. In Sections 3.2 and 3.3 non-adiabatic, and adiabatic treatments are introduced to simulate the optical spectra of exciton and biexciton in interaction with LO phonons.

3.1 Quantum dots models

3.1.1 Spherical quantum dot

Within the effective mass approximation, following (Cheche, et. al., 2005) a spherical model is considered for the case of size-quantized energies of QD (or equivalently, QD with

dimension smaller than its corresponding exciton Bohr radius, (Hanamura, 1988)). The confinement potential energy is $V_e(r_e)=0$ for $r_e \in [0, R_0]$, and $V_e(r_e)=V_{0e}$ for $r_e > R_0$ (similar equation is written for holes by replacing r_e by r_h); R_0 is the QD radius. The single-particle wave function is the product $\varphi_{nlm}(\mathbf{r})=R_{nl}(r)Y_{lm}(\theta, \varphi)$, where $R_{nl}(r)$ is the radial function and $Y_{lm}(\theta, \varphi)$ is the spherical harmonics function. By using the second quantization language, and disregarding the spin dependence, the electron-hole pair (EHP) state may be written as (Takagahara, 1993) $|f\rangle \rightarrow |\varphi_{ab}\rangle = \int d\mathbf{r}_e d\mathbf{r}_h \varphi_a(\mathbf{r}_e) \varphi_b(\mathbf{r}_h) a_e^{c+} a_h^v |0\rangle$, where a_e^{c+} (a_h^v) are the creation (annihilation) fermionic operator of an electron in the conduction band at \mathbf{r}_e (valence band at \mathbf{r}_h) and a (b) holds for the set of quantum numbers n_e, l_e, m_e (n_h, l_h, m_h) of electrons (holes). The single particle states composing the EHPs are obtained by optical excitation and we need to find the optical selection rules that dictate the allowed transitions. In the linear response theory and long wave approximation the particle-radiation Hamiltonian for a carrier of charge Q and mass M is given by $H_{Q-R} = -Q(Mc)^{-1} \mathbf{A} \cdot \mathbf{P}$, where c is the speed of light, \mathbf{A} is the vector potential, and \mathbf{P} is the carrier momentum. For monochromatic field of frequency ω , amplitude E_0 , and direction of oscillation along the unit polarization vector $\boldsymbol{\varepsilon}$, the semi-classical EHP-radiation interaction form of H_{Q-R} reads

$$H_{EHP-R} = -eE_0(m_0\omega)^{-1} \boldsymbol{\varepsilon} \cdot \sum_{f \neq 0} \left[\langle 0 | \mathbf{P} | f \rangle B_f + \langle f | \mathbf{P} | 0 \rangle B_f^\dagger \right] \sin \omega t \equiv W \sin \omega t \quad (10.a)$$

where $\mathbf{P} \equiv \sum_i \mathbf{p}_i$ the total electronic momentum (with \mathbf{p}_i the electron momentum) and B_f^\dagger (B_f) the creation (annihilation) exciton operators. The EHPs are considered as being bosons (EHP spin is an integer), a valid approximation in the dilute limit of excitons. Using an appropriate definition of the momentum (Takagahara, 1993), $\mathbf{P} = \mathbf{p}_{cv}^0 \int d\mathbf{R} a_{\mathbf{R}}^{c+} a_{\mathbf{R}}^v + h.c.$, where \mathbf{p}_{cv}^0 is the momentum matrix element between the valence-band and the conduction-band at the Γ point and where \mathbf{R} suggests integration over unit cell vectors, one obtains the optical matrix element

$$\langle \varphi_{ab} | \mathbf{P} | 0 \rangle = \mathbf{p}_{cv}^0 \delta_{l_e l_h} \delta_{m_e m_h} \int_0^\infty dr r^2 R_{n_e l_e}(r) R_{n_h l_h}(r) \equiv \mathbf{p}_{cv}^0 \delta_{m_e m_h} A_{n_e n_h l}, \quad (10.b)$$

with $l_e = l_h = l$. Thus, one obtains that the optical selection rule requires $l_e = l_h$. The model takes into account the difference in the effective masses between the nano-sphere and its surroundings. Following (Chamberlain et. al., 1995), the expression of orthonormalized $R_{nl}(r)$ and the secular equation of energy are as follows

$$R_{nl}(r) = \sqrt{\frac{2}{R_0^3}} \left[j_l^2(x) k_{l-1}(y) k_{l+1}(y) - k_l^2(y) j_{l-1}(x) j_{l+1}(x) \right] \begin{cases} k_l(y) j_l(x r/R_0), & r < R_0 \\ j_l(x) k_l(y r/R_0), & r > R_0 \end{cases} \quad (11.a)$$

$$\mu_2 x k_l(y) j_l'(x) = \mu_1 y j_l(x) k_l'(y) \quad (11.b)$$

where $x = R_0 \sqrt{(2\mu_1 E_{n,l})/\hbar^2}$, $y = R_0 \sqrt{(2\mu_2 (V_0^c - E_{n,l}))/\hbar^2}$, k_l is the modified spherical Bessel functions, μ_1 (μ_2) is the effective mass in the dot (surrounding medium), V_0^c the band offset of the carriers, and n, l stand for n_e, l_e (electrons) or n_h, l_h (holes).

For GaAs microcrystallites embedded in AlAs matrix, the compound discussed as an application, we use the parameters of material from (Menéndez et. al., 1997) : the GaAs energy gap $E_g = 1.5177$ eV, the GaAs (AlAs) electron effective mass $\mu_e/m_0 = 0.0665$ ($\mu_e/m_0 = 0.124$), the hole effective mass $\mu_h/m_0 = 0.45$ ($\mu_h/m_0 = 0.5$), the conduction band offset $V_0^c = 0.968$ eV, and the valence band offset $V_0^h = 0.6543$ eV; m_0 is the electron mass. The energy spectrum is obtained from Eqs. (11.a, b), and the EHP energy $E_{n_e, l_e; n_h, l_h} = E_g + E_{n_e, l_e} + E_{n_h, l_h}$ is computed as a function of the QD radius and shown in Fig. 3. Some particular levels are labeled by the set of quantum numbers, $(n_e, l_e, m_e; n_h, l_h, m_h)$ as follows: $A_0 \rightarrow (1,0,0;1,0,0)$, $B \rightarrow (1,0,0;1,1, m_h)$ - dark level, $C \rightarrow (1,0,0;1,2, m_h)$ - dark level, $D_0 \rightarrow (1,0,0;2,0,0)$, $E \rightarrow (1,1, m_e; 1,0,0)$ -dark level, $F \rightarrow (1,0,0;2,1, m_h)$ -dark level, $G_0 \rightarrow (1,1, m_e; 1,1, m_h)$. Based on the distribution of energy levels and taking into account the exciton Bohr radius (larger than 100\AA), we consider $R_0 = 50 \text{\AA}$ as a reasonable upper-limit for neglecting the Coulombic interaction. On the other hand, possible phonon mixing effect could manifest starting with $R_0 \approx 23 \text{\AA}$ (see the ellipse mark at Fig. 3), between the optically active level G_0 and the dark level F . But, the phonon-assisted transition between G_0 and D_0 is improbable (at least in the low temperature limit) because for the intermediate transfer, $E \rightarrow D_0$, $(E_E - E_{D_0})/\hbar\omega_0 = 3.37$ (the LO phonon energy $\hbar\omega_0 = 36.2\text{meV}$). For the first two optically active levels, the adiabatic treatment is safe for $R_0 < 22 \text{\AA}$ and may be accepted as satisfactory for $R_0 < 32 \text{\AA}$, beyond which the dark level C appears.

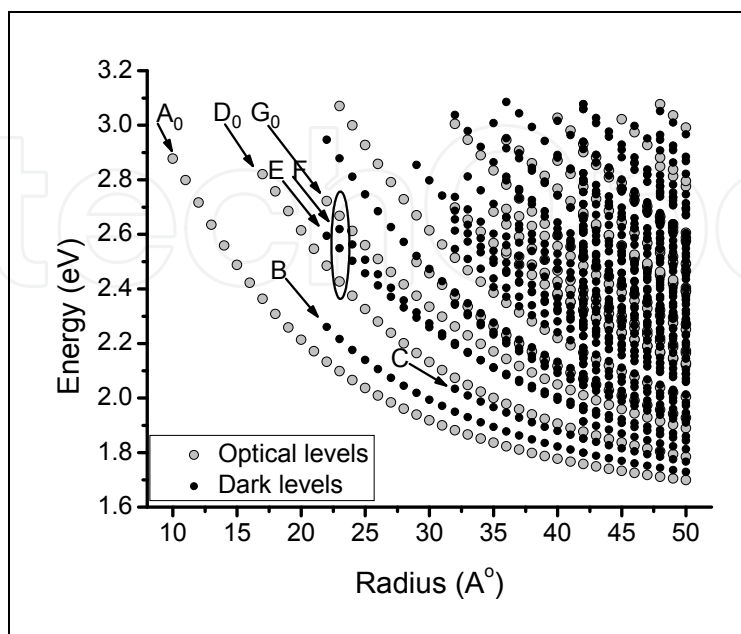


Fig. 3. The energy spectrum of small spherical GaAs/AlAs QDs.

3.1.2 Configurational interaction approach for cylindrical QDs

The energy levels of the exciton complexes can be obtained by the configurational interaction method (Hawrylak, 1999). Following (Cheche, 2009) we will describe a configurational interaction-based model for cylindrical semiconductor QDs. In the effective mass approximation the electron single particle wave function of QD can be approximated as the spin-orbital product (Haug & Koch, 1993) $\phi_{\alpha\sigma}(\mathbf{r}) = u_{\sigma}(\mathbf{r})\varphi_{\alpha}(\mathbf{r})$, where \mathbf{r} is the carrier position vector. $\varphi_{\alpha}(\mathbf{r})$ is the envelope function, and $u_{\sigma}(\mathbf{r})$ is the periodical Bloch function at Γ point with spin dependence included. The same is valid for holes by replacing, notation wise, e by h , α by β , and σ by τ . σ and τ are the z -projections of the Bloch angular momentum, with $\sigma = \pm 1/2$ and $\tau = \pm 3/2, \pm 1/2$. By disregarding the band-mixing, we safely assume that the topmost states are formed from degenerate heavy-hole states, that is, $\tau = \pm 3/2$. With ρ, z, φ , cylindrical coordinates, we consider for the conduction electrons the confining potential made up of the in-plane parabolic potential $V_{\parallel}^e(\rho) = \mu_e / (2\omega_e^2 \rho^2)$ and vertical potential, $V_{\perp}^e(z) = 0$ for $|z| \leq L/2$ and $V_{\perp}^e(z) = V_b^e$ otherwise. The single-particle Hamiltonian, $H_e = H_{e\rho} + H_{ez}$, has the components

$$H_{e\rho} = -\frac{\hbar^2}{2\mu_e} \left[\frac{1}{\rho} \frac{\partial}{\partial \rho} \left(\rho \frac{\partial}{\partial \rho} \right) \right] + V_{\parallel}^e(\rho), \quad H_{ez} = -\frac{\hbar^2}{2\mu_e} \frac{\partial^2}{\partial z^2} + V_{\perp}^e(z) \quad (12.a)$$

The corresponding Schrödinger equations read, $H_{e\rho}\psi(\rho, \varphi) = \varepsilon_{\rho\varphi}^e \psi(\rho, \varphi)$, and $H_{ez}\xi(z) = \varepsilon_z^e \xi(z)$. The electronic envelope wave functions $\varphi(\mathbf{r})$ is given by the product $\psi(\rho, \varphi)\xi(z)$, and has the concrete expression, $\varphi_{\alpha}(\mathbf{r}) = (2\pi)^{-1/2} e^{im_e\varphi} R_{n_e, m_e}(\rho) \xi_1^e(z)$, where α holds for the set of quantum numbers (n_e, m_e, i) . For QD sufficiently narrow we may consider $i=1$ level only, and take the approximate wave function of the first state in z direction as, $\xi_1^e(z) = (2/L_e)^{1/2} \cos(\pi z/L_e)$, where $L_e = L \left[1 + 2\hbar / (L\sqrt{2\mu_e V_b^e}) \right]$ is the effective QD height including the band-offset, L is the QD height (Barker et. al., 1991). Thus, for the electron, the envelope wave function reads

$$\begin{aligned} \varphi_{\alpha}(\mathbf{r}) &= e^{im_e\varphi} (2\pi)^{-1/2} [(2n_e!)/(n_e + |m_e|)!]^{-1/2} (\rho/l_e)^{|m_e|} e^{-\frac{\rho^2}{2l_e^2}} l_e^{-1} L_{n_e}^{|m_e|}(\rho^2/l_e^2) \xi_1(z) \\ &\equiv (2\pi)^{-1/2} e^{im_e\varphi} R_{\alpha}(\rho) \xi_1(z) \end{aligned} \quad (12.b)$$

with $L_{n_e}^{|m_e|}$ denoting Laguerre polynomials, $n_e = 0, 1, 2, \dots$, $m_e = 0, \pm 1, \pm 2, \dots$, $l_e = \sqrt{\hbar / (\mu_e \omega_e)}$, and α re-denoting the set (n_e, m_e) for $i=1$. The corresponding energy states are obtained as $\varepsilon_{\alpha} = \varepsilon_{n_e m_e} + \varepsilon_{1ez}$, where $\varepsilon_{n_e m_e}$ and ε_{1ez} are the quantized values of $\varepsilon_{\rho\varphi}^e$ and ε_z^e , respectively. The quantized energy for the in-plane motion is $\varepsilon_{n_e m_e} = (2n_e + |m_e| + 1)\hbar\omega_e$. The same considerations are valid for holes, by considering the effective mass in z direction, μ_{hz} , and the in-plane effective mass $\mu_{h\rho}$. An immediate analysis shows the spin-orbitals set

$\{\phi_{\alpha\sigma}(\mathbf{r}), \phi_{\beta\tau}(\mathbf{r})\}$ is orthonormal. The integrals involving spin-orbitals are solved by the usual decomposition in a product of two integrals, one over the space of the unit cells position vectors for slowly varying functions, and the other one over the unit cell space for rapidly varying functions. Thus, for example, one obtains, $\langle \phi_{\alpha\sigma} | \phi_{\beta\tau} \rangle = \langle \varphi_{\alpha} | \varphi_{\beta} \rangle_{all\ space} \langle u_{\sigma} | u_{\tau} \rangle_{\Omega_0} = 0$ from the orthonormality of the periodical Bloch functions (the indices show the volume of integration, with Ω_0 the unit cell volume). For such orthonormal basis set two equivalent ways, the language of the second quantization, and the technique of the determinantal states can be used to describe the energy structure of the system.

Next, we adopt the creation (annihilation) fermion operators, $c_{\alpha\sigma}^+$ ($c_{\alpha\sigma}$) for electron in conduction band, and $h_{\beta\tau}^+$ ($h_{\beta\tau}$) for hole in valence band; they create (annihilate) the carrier with spin projection σ for electrons and τ for holes. Considering negligible the piezoelectricity and the band-mixing effects, and disregarding the electron-hole exchange interaction, the QD Hamiltonian reads

$$H_D = \sum_{\alpha,\sigma} \varepsilon_{\alpha} c_{\alpha\sigma}^+ c_{\alpha\sigma} + \sum_{\beta,\tau} \varepsilon_{\beta} h_{\beta\tau}^+ h_{\beta\tau} + \frac{1}{2} \sum_{\substack{\alpha_1,\alpha_2,\alpha_3,\alpha_4 \\ \sigma_1,\sigma_2}} V_{\substack{\alpha_1\sigma_1,\alpha_2\sigma_2 \\ \alpha_3\sigma_1,\alpha_4\sigma_2}}^{ee} c_{\alpha_1\sigma_1}^+ c_{\alpha_2\sigma_2}^+ c_{\alpha_4\sigma_2} c_{\alpha_3\sigma_1} \\ + \frac{1}{2} \sum_{\substack{\beta_1,\beta_2,\beta_3,\beta_4 \\ \tau_1,\tau_2}} V_{\substack{\beta_1\tau_1,\beta_2\tau_2 \\ \beta_3\tau_1,\beta_4\tau_2}}^{hh} h_{\beta_1\tau_1}^+ h_{\beta_2\tau_2}^+ h_{\beta_4\tau_2} h_{\beta_3\tau_1} + \sum_{\substack{\alpha_1,\beta_1,\alpha_2,\beta_2 \\ \sigma_1,\tau_1,\sigma_2,\tau_2}} V_{\substack{\alpha_1\sigma_1,\beta_1\tau_1 \\ \alpha_2\sigma_2,\beta_2\tau_2}}^{eh} c_{\alpha_1\sigma_1}^+ h_{\beta_1\tau_1}^+ h_{\beta_2\tau_2} c_{\alpha_2\sigma_2} \quad , (13)$$

where the first, second, third, fourth, and fifth terms of right side stand for electrons, holes, electron-electron, hole-hole, and electron-hole Coulomb interactions, respectively.

Regarding the significance of terms in Eq. (13), we have (Takagahara, 1999)

$$V_{\substack{\alpha_1\sigma_1,\beta_1\tau_1 \\ \alpha_2\sigma_2,\beta_2\tau_2}}^{eh} = -\delta_{\sigma_1\sigma_2} \delta_{\tau_1\tau_2} \iint_V d\mathbf{R}_e d\mathbf{R}_h \varphi_{\alpha_1}^*(\mathbf{R}_e) \varphi_{\beta_1}^*(\mathbf{R}_h) \frac{e^2}{4\pi\varepsilon|\mathbf{p}_e - \mathbf{p}_h|} \varphi_{\alpha_2}(\mathbf{R}_e) \varphi_{\beta_2}(\mathbf{R}_h), \quad (14)$$

where V is the volume of QD. Similar expressions hold for $V_{\substack{\alpha_1\sigma_1,\alpha_2\sigma_2 \\ \alpha_3\sigma_1,\alpha_4\sigma_2}}^{ee}$ and $V_{\substack{\beta_1\tau_1,\beta_2\tau_2 \\ \beta_3\tau_1,\beta_4\tau_2}}^{hh}$; the capital bold characters suggest integration over the 'coarse-grained' space of the unit cell position vectors. In Eq. (14), we considered an in-plane Coulombic interaction, with \mathbf{p} the in-plane position vector. After integration over z , which gives unity, one obtains an integral over \mathbf{p} only. Integral from Eq. (14) is solved as follows. The potential is written as a two-dimensional Fourier transform, $v(|\mathbf{p}_e - \mathbf{p}_h|) \equiv 1/|\mathbf{p}_e - \mathbf{p}_h| = \int d\mathbf{q} v(\mathbf{q}) e^{i\mathbf{q}\cdot(\mathbf{p}_e - \mathbf{p}_h)}$, and the inverse Fourier transform reads

$$v(\mathbf{q}) = \frac{1}{4\pi^2} \int d\mathbf{p} v(\rho) e^{-i\mathbf{q}\cdot\mathbf{p}} = \frac{1}{4\pi^2} \int_0^{\infty} d\rho \rho \int_0^{2\pi} d\varphi \frac{1}{\rho} e^{-iq\rho \cos\varphi} \\ = \frac{1}{4\pi^2} \int_0^{\infty} d\rho \int_0^{2\pi} d\varphi \sum_{m=-\infty}^{\infty} i^m e^{im\varphi} J_m(q\rho) = \int_0^{\infty} d\rho J_0(q\rho) = \frac{1}{2\pi q}$$

where φ is the angle between \mathbf{q} and $\boldsymbol{\rho}$. Using these expressions we write in Eq. (14)

$$\begin{aligned} & \iint_V d\mathbf{R}_e d\mathbf{R}_h \varphi_{\alpha_1}^*(\mathbf{R}_e) \varphi_{\beta_1}^*(\mathbf{R}_h) \frac{1}{|\boldsymbol{\rho}_e - \boldsymbol{\rho}_h|} \varphi_{\alpha_2}(\mathbf{R}_e) \varphi_{\beta_2}(\mathbf{R}_h) \\ &= \int_0^\infty dq \int_0^{2\pi} d\varphi \int_{S_0} d\boldsymbol{\rho}_e e^{i(m_{e2} - m_{e1})\varphi} R_{\alpha_1}(\rho_e) e^{i\mathbf{q}\cdot\boldsymbol{\rho}_e} R_{\alpha_2}(\rho_e) \int_{S_0} d\boldsymbol{\rho}_h (2\pi)^{-1} e^{-i(m_{h2} - m_{h1})\varphi} R_{\beta_1}(\rho_h) e^{-i\mathbf{q}\cdot\boldsymbol{\rho}_h} R_{\beta_2}(\rho_h) \end{aligned}$$

where S_0 is the cylinder base surface. Next, we introduce

$$I_{\alpha_1\alpha_2}^e(\mathbf{q}) = \frac{1}{2\pi} \int_{S_0} d\boldsymbol{\rho} e^{i(m_{e2} - m_{e1})\varphi} R_{\alpha_1}(\rho) e^{i\mathbf{q}\cdot\boldsymbol{\rho}} R_{\alpha_2}(\rho) = \frac{1}{2\pi} \int_0^\infty d\rho \rho R_{\alpha_1}(\rho) R_{\alpha_2}(\rho) \int_0^{2\pi} d\varphi e^{i(m_{e2} - m_{e1})\varphi} e^{iq\rho \cos\varphi}$$

and by using $\exp(iz \cos \varphi) = \sum_{p=-\infty}^\infty i^p J_p(z) \exp(ip\varphi)$, one obtains

$$I_{\alpha_1\alpha_2}^e(\mathbf{q}) = \sum_{p=-\infty}^\infty \int_0^\infty d\rho \rho R_{\alpha_1}(\rho) R_{\alpha_2}(\rho) \delta_{p, m_{e2} - m_{e1}} i^p J_p(q\rho) = i^{m_{e2} - m_{e1}} \int_0^\infty d\rho \rho R_{\alpha_1}(\rho) R_{\alpha_2}(\rho) J_{m_{e2} - m_{e1}}(q\rho)$$

Similarly, for holes, $I_{\beta_1\beta_2}^h(\mathbf{q}) = i^{-(m_{h2} - m_{h1})} \int_0^\infty d\rho \rho R_{\beta_1}(\rho) R_{\beta_2}(\rho) J_{m_{h1} - m_{h2}}(q\rho)$. Conservation of the angular momentum in z direction requires $m_{e1} = -m_{h1}$, and $m_{e2} = -m_{h2}$. For Eq. (14),

after an integration over φ , we have $V_{\substack{n,m,\sigma_1;n,-m,\tau_1 \\ n',m',\sigma_2;n',-m'\tau_2}}^{eh} = -\delta_{\sigma_1\sigma_2} \delta_{\tau_1\tau_2} \mathbf{e}^2 (4\pi\epsilon)^{-1} \times \int_0^\infty dq I_{n,m;n',m'}^e(\mathbf{q}) I_{n',-m;n,-m'}^h(\mathbf{q})$; such integrals have analytic solutions. General solutions of Coulombic integral for in-plane interaction can be found in (Jacak et. al., 1998).

The exciton state $|X_f^1\rangle$ is written as a linear combination of determinantal states,

$$|X_f^1\rangle = \sum_{\alpha\sigma,\beta\tau} C_{\alpha\sigma,\beta\tau}^f c_{\alpha\sigma}^+ c_{\beta\tau}^+ h_{\beta\tau}^+ |0\rangle \equiv X_f^{1+} |0\rangle, \tag{15.a}$$

with $|0\rangle$ standing for the exciton vacuum state (no excitons), the ground state (VS) of the system. Similarly, the biexciton $|X_f^2\rangle$ state is written as linear combinations of determinantal states that differ of the VS by two of the spin-orbitals

$$|X_f^2\rangle = \sum_{\substack{\alpha_1\sigma_1,\alpha_2\sigma_2 \\ \beta_1\tau_1,\beta_2\tau_2}} C_{\alpha_1\sigma_1,\alpha_2\sigma_2,\beta_1\tau_1,\beta_2\tau_2}^f c_{\alpha_1\sigma_1}^+ c_{\alpha_2\sigma_2}^+ h_{\beta_1\tau_1}^+ h_{\beta_2\tau_2}^+ |0\rangle \equiv X_f^{2+} |0\rangle. \tag{15.b}$$

The eigen-problem for exciton and biexcitons is solved through the equations $H_D |X_f^1\rangle = \epsilon_f^{(1)} |X_f^1\rangle$, and $H_D |X_f^2\rangle = \epsilon_f^{(2)} |X_f^2\rangle$. Their corresponding secular equations allow obtaining the eigenvalues and eigenfunctions corresponding to the exciton and biexciton states. It is worth noting that the electron-electron and hole-hole Hamiltonians from Eq. (13) have no contribution to the secular equation associated to the exciton eigen-problem; the product of fermionic operators resulting from these Hamiltonians and from the exciton state forms sequence of operators which when acting on the VS gives zero.

Referring to the determinantal state technique, the VS is written as the ground-state Slater determinant $\Phi_0(\mathbf{r}_1, \tau_1, \dots, \mathbf{r}_v, \tau, \dots, \mathbf{r}_N, \tau_N) = \mathbf{A} [\phi_{\beta_1 \tau_1}(\mathbf{r}_1), \dots, \phi_{\beta_\tau}(\mathbf{r}_v), \dots, \phi_{\beta_N \tau_N}(\mathbf{r}_N)]$, where N is the total number of electrons in the system, and \mathbf{A} is the antisymmetrizing operator. A single-substitution Slater determinant is written by promoting an electron from the occupied valence state $\phi_{\beta_\tau}(\mathbf{r}_v)$ to the unoccupied conduction state $\phi_{\alpha\sigma}(\mathbf{r}_v)$

$$\Phi_{\beta_\tau, \alpha\sigma}(\mathbf{r}_1, \tau_1, \dots, \mathbf{r}_v, \sigma, \dots, \mathbf{r}_N, \tau_N) = \mathbf{A} [\phi_{\beta_1 \tau_1}(\mathbf{r}_1), \dots, \phi_{\alpha\sigma}(\mathbf{r}_v), \dots, \phi_{\beta_N \tau_N}(\mathbf{r}_N)].$$

The following equivalence between the single-substitution Slater determinant and configurations written in the language of the second quantization holds:

$$\Phi_{\beta_\tau, \alpha\sigma}(\mathbf{r}_1, \tau_1, \dots, \mathbf{r}_v, \sigma, \dots, \mathbf{r}_N, \tau_N) \leftrightarrow c_{\alpha\sigma}^+ h_{\beta_\tau}^+ |0\rangle.$$

Taking the advantage of the determinantal states, we search for the optical selection rules that dictate the optically active pair states to be used in the linear combination from Eqs. (15.a, b). The radiation field is modeled as a single mode of polarized plane wave. In the limit of linear response theory and long-wave approximation, the semiclassical particle-field interaction Hamiltonian, for transitions $|X^m\rangle \leftrightarrow |X^{m-1}\rangle$ (with $|X^0\rangle \equiv |0\rangle$) is written as $H_{X^m-R} = eE_0(m_0\omega)^{-1} \boldsymbol{\varepsilon} \cdot \mathbf{P}_{X^m}$, where the momentum operator is $\mathbf{P}_{X^m} = \sum_{f,i} |X_f^m\rangle \langle X_f^m| \mathbf{p}_i |X_f^{m-1}\rangle \langle X_f^{m-1}| + h.c.$, with \mathbf{p}_i the momentum of the i electron and summation is done over all the electrons of the system and (multi)exciton states. Then, by using the algebra of determinantal states (Grosso & Parravicini, 2000), we have:

$$\langle X_f^1 | \sum_i \mathbf{p}_i | 0 \rangle = \sum_{\alpha\sigma, \beta\tau} C_{\alpha\sigma, \beta\tau}^{f*} \langle 0 | h_{\beta\tau} c_{\alpha\sigma} \sum_i \mathbf{p}_i | 0 \rangle = \sum_{\alpha\sigma, \beta\tau} C_{\alpha\sigma, \beta\tau}^{f*} \langle \phi_{\alpha\sigma} | \mathbf{p} | \phi_{\beta\tau} \rangle, \quad (16.a)$$

$$\begin{aligned} \langle X_f^2 | \sum_i \mathbf{p}_i | X_f^1 \rangle &= \sum_{\substack{\alpha_1 \sigma_1, \alpha_2 \sigma_2 \\ \beta_1 \tau_1, \beta_2 \tau_2}} C_{\alpha_1 \sigma_1, \alpha_2 \sigma_2}^{i*} \langle 0 | h_{\beta_2 \tau_2} h_{\beta_1 \tau_1} c_{\alpha_2 \sigma_2} c_{\alpha_1 \sigma_1} \sum_i \mathbf{p}_i \sum_{\alpha\sigma, \beta\tau} C_{\alpha\sigma, \beta\tau}^f c_{\alpha\sigma}^+ h_{\beta\tau}^+ | 0 \rangle \\ &= \sum_{\substack{\alpha\sigma, \alpha_1 \sigma_1 \\ \beta\tau, \beta_1 \tau_1}} C_{\alpha\sigma, \alpha_1 \sigma_1}^{i*} C_{\alpha\sigma, \beta\tau}^f \langle \phi_{\alpha_1 \sigma_1} | \mathbf{p} | \phi_{\beta_1 \tau_1} \rangle \end{aligned} \quad (16.b)$$

If we make use of the fact that the envelope functions vary relatively slowly over regions of the size of a unit cell, with $\mathbf{p} = -i\hbar\nabla$, we can write the integral

$$\begin{aligned} \langle \phi_{\alpha\sigma} | \mathbf{p} | \phi_{\beta\tau} \rangle &= \int_{\Omega_0} d\mathbf{r} u_{\sigma}^{e*}(\mathbf{r}) \mathbf{p} u_{\tau}^h(\mathbf{r}) \int_{all\ space} d\mathbf{r} \varphi_{\alpha}^*(\mathbf{r}) \varphi_{\beta}(\mathbf{r}) \\ &+ \int_{\Omega_0} d\mathbf{r} u_{\sigma}^{e*}(\mathbf{r}) u_{\tau}^h(\mathbf{r}) \int_{all\ space} d\mathbf{r} \varphi_{\alpha}^*(\mathbf{r}) \mathbf{p} \varphi_{\beta}(\mathbf{r}) \equiv \mathbf{p}_{cv}^0 \int_{all\ space} d\mathbf{r} \varphi_{\alpha}^*(\mathbf{r}) \varphi_{\beta}(\mathbf{r}) \end{aligned} \quad (16.c)$$

The second integral over unit cell of orthogonal Bloch periodical functions vanishes and Eq. (16.c) is in accordance with Eq. (10.b). Passing from the momentum matrix element to the dipole matrix element in Eqs. (16.a, b) we obtain the following (multi)exciton-field interaction Hamiltonians:

$$H_{X^1-R} = i\mathbf{e}E_0\omega^{-1}\sum_f\sum_{\alpha\sigma,\beta\tau}C_{\alpha\sigma,\beta\tau}^{f*}\omega_{\alpha\beta}\langle\phi_{\alpha\sigma}|\boldsymbol{\varepsilon}\cdot\mathbf{r}|\phi_{\beta\tau}\rangle X_f^{1+} - h.c. = \omega^{-1}\sum_f\left(C^f X_f^{1+} + h.c.\right), \quad (17.a)$$

and

$$H_{X^2-R} = iE_0\mathbf{e}(m_0\omega)^{-1}\left(\sum_{i,f}\sum_{\substack{\alpha\sigma,\alpha_1\sigma_1, \\ \beta\tau,\beta_1\tau_1}}C_{\alpha\sigma,\alpha_1\sigma_1}^{i*}C_{\beta\tau,\beta_1\tau_1}^f\omega_{\alpha_1\beta_1}\langle\phi_{\alpha_1\sigma_1}|\boldsymbol{\varepsilon}\cdot\mathbf{r}|\phi_{\beta_1\tau_1}\rangle X_i^{2+} X_f^1 - h.c.\right) \\ \equiv \omega^{-1}\sum_{i,f}\left(C^{if} X_i^{2+} X_f^1 + h.c.\right). \quad (17.b)$$

We used the notations: $\omega_{\alpha\beta} = (\varepsilon_\alpha^e - \varepsilon_\beta^h)/\hbar$, and ω , E_0 for frequency, amplitude of the radiation field, respectively. We also introduced $X_f^{1+} = |X_f^1\rangle\langle 0|$, $X_f^{2+} = |X_f^2\rangle\langle 0|$, $X_i^{2+} X_f^1 = |X_i^2\rangle\langle X_f^1|$. The optical selection rules for interband transitions are obtained from the $\boldsymbol{\varepsilon}\cdot\mathbf{r}$ matrix element. Thus

$$\langle\phi_{\alpha\sigma}|\boldsymbol{\varepsilon}\cdot\mathbf{r}|\phi_{\beta\tau}\rangle = \frac{1}{\Omega_0}\boldsymbol{\varepsilon}\cdot\int_{\Omega_0}d\mathbf{r}u_\sigma^{e*}(\mathbf{r})\mathbf{r}u_\tau^h(\mathbf{r})\int_{\text{all space}}d\mathbf{R}\varphi_\alpha^*(\mathbf{R})\varphi_\beta(\mathbf{R}), \quad (18)$$

By writing: i) the periodical Bloch functions at the Γ point, $u_{a^j}(\mathbf{r}) = \zeta_{a^j}(r)\chi_{a^j}(\theta, \varphi)$, where $j = e, h$, and $a^e = \pm 1/2$, $a^h = \pm 3/2$, as the following spinors (Merzbacher, 1988): $\chi_{1/2,1/2}^e(\theta, \varphi) = Y_0^0(\theta, \varphi)|\uparrow\rangle$, $\chi_{1/2,-1/2}^e(\theta, \varphi) = Y_0^0(\theta, \varphi)|\downarrow\rangle$, $\chi_{3/2,3/2}^h(\theta, \varphi) = Y_1^1(\theta, \varphi)|\uparrow\rangle$, $\chi_{3/2,-3/2}^h(\theta, \varphi) = Y_1^{-1}(\theta, \varphi)|\downarrow\rangle$, and ii) the position vector for light propagating in z direction, $\mathbf{r} = r(-Y_1^1\hat{\mathbf{e}}_- + Y_1^{-1}\hat{\mathbf{e}}_+)$ with $\hat{\mathbf{e}}_-$, $\hat{\mathbf{e}}_+$ the light helicity unit polarization vectors, we obtain the spin selection rules for the configurations. Thus, one finds that for linearly polarized light propagating in z direction, the only non-vanishing matrix elements involving the heavy-hole states correspond to the transitions $\sigma = 1/2 \leftrightarrow \tau = 3/2$ and $\sigma = -1/2 \leftrightarrow \tau = -3/2$. This result is guiding us in choosing the optically active configurations when using the configurational interaction method to obtain the energy structure of QD.

To obtain spin-polarized excitons, the linearly polarized light is used for photoexcitation. The nonequilibrium spin decays due to both carrier recombination and spin relaxation. Accordingly to (Paillard et al., 2001), and (Sénès et al., 2005), who studied polarization dynamics with linearly polarized light in InAs/GaAs self-assembled QD under (quasi)resonant excitation, following excitation the electron and hole spin states remain stable during the exciton lifetime for low temperatures. This is the case we assumed for the present discussion. Linearly polarized light is a linear combination of circularly polarized light with positive and negative helicity (Zutić, et. al, 2004), consequently, the configurations are obtained by respecting the optical selection rules for interband transitions for circularly polarized light with both positive and negative helicity.

Accordingly to our assumption that the electron and hole spins remain stable during the exciton lifetime the appearance of dark states (states with opposite spins of the electron and

hole of a pair) is less probable, and we disregard them. Within the configurational interaction method we consider a limited number of states generated by the two lowest shells s and p configurations optically active, that is the pair states having $n_e = n_h = 0$, and $m_e = -m_h = 0, \pm 1$, as shown in Fig. 4. In Fig. 4, the filled (empty) triangles represent electrons (holes) of Bloch angular spin projection $\pm 1/2$ ($\pm 3/2$). The quantum numbers $(n_e, m_e), (n_h, m_h)$ are shown for the single states.

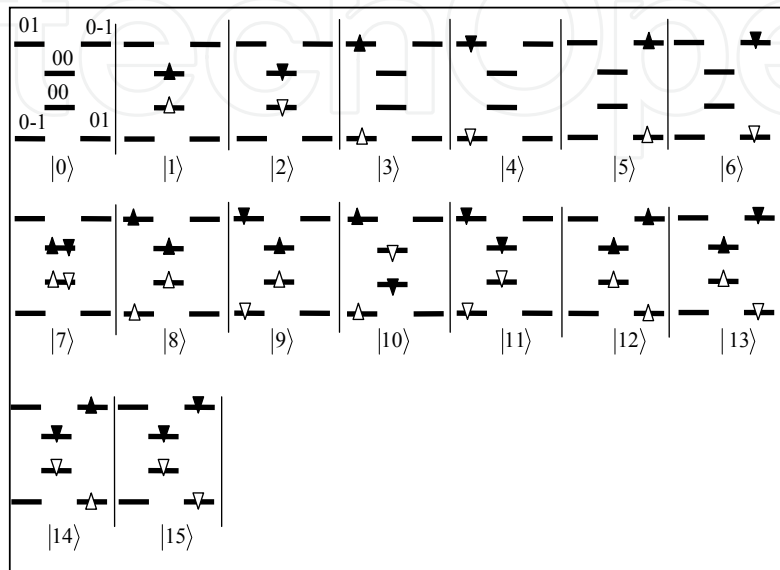


Fig. 4. Vacuum state, exciton and biexciton bright states with linearly polarized light.

Next, we apply the model to cylindrical InAs/AlAs QD. We use the following material parameters taking into account the presence of lattice mismatch strain: a) For InAs $\mu_e = 0.04m_0$, $\mu_{hz} = 0.41m_0$, $\mu_{hp} = 0.04m_0$, $\epsilon_0/\epsilon_v = 11.74$, $\epsilon_\infty/\epsilon_v = 15.54$ (ϵ_v is the vacuum dielectric permittivity), $\hbar\omega_0 = 29.5\text{meV}$, and the energy gap, $E_g = 0.824\text{eV}$; b) For the InAs/AlAs the band-offsets are considered as $V_b^e = 1.5\text{eV}$, $V_b^h = 0.75\text{eV}$ (Vurgaftman et. al., 2001); c) For the value of QD height $L=2.3\text{nm}$ which is considered, we find 1 electron and 3 hole levels in the quantum-well in the z direction. By setting $\hbar\omega_e = 0.065\text{eV}$ and $\omega_e/\omega_h = 3$, (according to the literature (Hawrylak, 1999; Shumway et. al., 2001) the exciton and biexciton eigenvalues obtained for this material parameters are as follows, $\epsilon_1^{(1)} = 1.5792\text{eV}$, $\epsilon_2^{(1)} = 1.6696\text{eV}$, $\epsilon_3^{(1)} = 1.6736\text{eV}$ (all three two-fold degenerate), $\epsilon_1^{(2)} = 3.1617\text{eV}$, $\epsilon_2^{(2)} = 3.2429\text{eV}$ -three-fold degenerate, $\epsilon_3^{(2)} = 3.24345\text{eV}$, and $\epsilon_4^{(2)} = 3.24719\text{eV}$ -four-fold degenerate. Consequently, the inter-level bi/exciton energy is not close of the LO phonon energy and the mixing of the bi/exciton states by phonons is absent.

3.2 Confined optical phonons in semiconductor quantum dots

There are several theoretical models which investigates the optical phonon modes in semiconductors with low dimensionality. Generally, the LO phonons are considered as the main contributors to the electron-phonon coupling in polar semiconductors in the relaxation

processes. Based on the continuum approach for long-wavelength optical phonons of (Born & Huang, 1998), macroscopic approaches, such as the dielectric continuum (DC) model (Fuchs & Kliewer, 1965; Klein et. al. 1990)), the multimode DC model (Klimin et. al., 1995), the mixed mechanical-electrostatic model (Roca et. al., 1994), and the hydrodynamic model (Ridley, 1989) have been developed. Microscopic approaches have also been proposed (Huang & Zhu, 1988; Rucker et. al., 1991).

The shape of QD plays a major role in setting the type of confined phonon modes and the strength of the exciton-phonon interaction. For spherical QD, the problem of the polaron was the most intensive studied case. One of the conclusions of the studies is that the inside QD, the electron-surface optical phonon interaction is absent (Melnikov & Fowler, 2001). Physically, this can be explained within the adiabatic picture: the electron is fast oscillating and in the ground state, which has a spherical symmetry of the charge distribution, the average surface ionic polarization charge is zero. For other shapes, the geometry itself brings additional complications in the study of the exciton-phonon interaction. Next, we extrapolate the above observation regarding the absence of electron-surface LO phonon interaction in spherical QD to the cylindrical shape case. The approximation is supported by the results obtained by (Cheche et. al., 2011), where calculus shows the exciton-bulk LO phonon interaction in such cylindrical QDs is dominant. Consequently, in the analysis of the optical spectra from the next sections, we consider the bulk LO phonons as the main contributors to the (multi)exciton-LO phonon interaction.

3.3 Optical spectra of spherical semiconductor quantum dots. A non-adiabatic treatment

Non-adiabatic treatments, necessary when the electron-hole pair (EHP) level spacing is comparable to the LO phonon energy, have been proposed (Cheche et. al., 2005; Fomin et. al., 1998; Takagahara, 1999; Vasilevskiy et. al., 2004; Verzelen et. al., 2002). Following (Cheche et. al. 2005; Cheche & Chang, 2005) in this section a non-adiabatic treatment of optical absorption in QDs is presented. The theoretical tool we develop: i) confirms existence of resonances accompanying the LO satellites in the optical spectra; ii) explains the temperature effect on the optical spectra. The Hamiltonian of the EHP-LO phonon reservoir we use is described by an extension of the Huang-Rhys model of F centers of the type described in Section 2.2,

$$H = H_{EHP} + H_{ph} + H_{EHP-ph}, \quad (19)$$

where $H_{EHP} \equiv \sum_f E_f B_f^+ B_f$, $H_{ph} \equiv \sum_{\mathbf{q}} \hbar \omega_{\mathbf{q}} b_{\mathbf{q}}^+ b_{\mathbf{q}}$, $H_{EHP-ph} \equiv \sum_{\mathbf{q}, f, f'} M_{\mathbf{q}}^{ff'} B_f^+ B_{f'} (b_{\mathbf{q}} + b_{-\mathbf{q}}^+)$, B_f^+ (B_f) are the exciton operators already introduced in section 3.1.1, $b_{\mathbf{q}}^+$ ($b_{\mathbf{q}}$) are the bosonic creation (annihilation) operators of the phonons of mode \mathbf{q} , $M_{\mathbf{q}}^{ff'} \equiv \langle f | M_{\mathbf{q}} | f' \rangle$ is the coupling matrix element, $\omega_{\mathbf{q}}$ is the frequency of the phonon mode with wave vector \mathbf{q} , and E_f ($|f\rangle$) are the EHP eigenvalues (eigenstates) of the exciton system. The absorption coefficient for a single QD is given by (Mittin et al., 1999)

$$\alpha(\omega) = \frac{2\pi\hbar\omega}{ncE_0^2V_0} R_{abs} \quad (20.a)$$

where ω is the frequency, E_0 is the amplitude of the monochromatic radiation field, n is the refractive index of the environment, V_0 is the absorptive volume, and R_{abs} is the radiation absorption rate. R_{abs} is calculated with the Fermi Golden Rule as follows.

$$R_{abs} = \frac{2\pi}{\hbar} A_V \sum_{GF} |W_{GF}|^2 \delta(\hbar\omega + E_G - E_F) \quad (20.b)$$

The average A_V involved by Eq. (20.b) means a quantum average over the finite number of the exciton states in the QD and a statistical average over the phonon modes at thermal equilibrium. In Eq. (20.b), E_G is the energy of the system in the ground state (no exciton) $|G\rangle = |0\rangle|\gamma\rangle$ ($|\gamma\rangle$ is the phonon state), E_F is the energy of the system in one of the exciton+phonons states $|F\rangle = |f;\varphi\rangle$ ($|f\rangle, |\varphi\rangle$ is the exciton, phonon state, respectively), and $W_{GF} = \langle G|W|F\rangle$ is the transition probability between the initial state $|G\rangle$ and the final state $|F\rangle$, with W from Eq. (10.a). Greek letters are used for phonon states, Latin letters for exciton states, and capital handwriting letters for all system. Eq. (20.b) can explicitly be written as follows

$$\begin{aligned} R_{abs} &= \frac{2\pi}{\hbar} Tr \left\{ \rho \sum_{GF} |W_{GF}|^2 \delta(\hbar\omega + E_G - E_F) \right\} \\ &= \frac{1}{\hbar^2} \int_{-\infty}^{\infty} dt e^{i\omega t} Tr \left\{ \rho \sum_G \langle G| e^{iH_{ph}/\hbar} W e^{-iH/\hbar} \left(\sum_F |F\rangle\langle F| + |G\rangle\langle G| \right) W |G\rangle \right\} \\ &= \frac{1}{\hbar^2} \int_{-\infty}^{\infty} dt e^{i\omega t} Tr \left\{ \rho \sum_G \langle G| e^{iH_{ph}/\hbar} W e^{-iH/\hbar} W |G\rangle \right\} = \frac{1}{\hbar^2} \int_{-\infty}^{\infty} dt e^{i\omega t} \langle \langle 0|\tilde{W}(t)W|0\rangle \rangle_0 \end{aligned} \quad (20.c)$$

where $\rho = \sum_{\nu} |\nu\rangle \rho_{\nu} \langle \nu|$ is the density matrix of the phonons, with $\rho_{\nu} = e^{-\beta E_{\nu}} / Tr(e^{-\beta H_{ph}})$ the probability of the phonon state $|\nu\rangle$ in the equilibrium statistical ensemble of the phonons, and $Tr\{A\} = \sum_{\nu} \langle \nu|A|\nu\rangle = \sum_{\nu} A_{\nu\nu}$, $\langle A \rangle_0 \equiv Tr\{\rho A\} = \sum_{\nu} \rho_{\nu} \langle \nu|A|\nu\rangle = \sum_{\nu} \rho_{\nu} A_{\nu\nu}$. The closure relation $\sum_F |F\rangle\langle F| + |G\rangle\langle G| = \mathbf{1}$ was used in the second equality of Eq. (20.c), where the operator $\sum_G |G\rangle\langle G| = \sum_{\mu} |0\rangle\langle \mu| \langle \mu| \langle 0|$, which has no effect on the matrix element was inserted. If using an adiabatic picture the state $|F\rangle$ is written as a product of states, $|F\rangle = |f;\varphi\rangle = |f\rangle|\varphi\rangle$, and the meaning of the closure relation is more transparent:

$$\sum_F |F\rangle\langle F| + |G\rangle\langle G| = \sum_{f,\nu} |f\rangle\langle \nu| \langle \nu| \langle f| + \sum_{\mu} |0\rangle\langle \mu| \langle \mu| \langle 0| = \left(\sum_f |f\rangle\langle f| + |0\rangle\langle 0| \right) \sum_{\nu} |\nu\rangle\langle \nu| = \mathbf{1}.$$

In Eq. (20.c), $\tilde{W}(t) = e^{iH_{ph}/\hbar} W e^{-iH/\hbar}$. Eqs. (20a-c) give

$$\alpha(\omega) = \frac{2\pi e^2}{ncm_0^2 \hbar \omega V_0} \int_{-\infty}^{\infty} dt e^{i\omega t} \langle \langle 0|\tilde{W}(t)W|0\rangle \rangle_0 \quad (21.a)$$

By using the bosonic commutation rules for creation and annihilation of EHP and phonons, the operator relation $e^{A+B} = e^A e^B e^{-[A,B]/2}$, we write Eq. (21.a) as follows:

$$\alpha(\omega) = \frac{2\pi e^2}{ncm_0^2 \hbar \omega V_0} \sum_{f, f' \neq 0} \left[P_{0f} P_{f'0} \int_{-\infty}^{\infty} dt \exp[i(\omega - \omega_f)t] \langle 0 | B_f \left\langle \hat{T} \exp \left[-\frac{i}{\hbar} \int_0^t dt_1 \tilde{V}(t_1) \right] \right\rangle_0 B_{f'}^\dagger | 0 \rangle \right] \quad (21.b)$$

where \hat{T} is the time-ordered operator, $\tilde{V}(t) = \exp(itH_0/\hbar) H_{EHP-ph} \exp(-itH_0/\hbar)$, $\left\langle \hat{T} \exp \left[-\frac{i}{\hbar} \int_0^t dt_1 \tilde{V}(t_1) \right] \right\rangle_0 \equiv \langle U(t) \rangle_0$, $H_0 \equiv H_{EHP} + H_{ph}$, $P_{0f} \equiv \langle 0 | (\boldsymbol{\varepsilon} \cdot \mathbf{P}) | f \rangle$, and $\mathbf{P} \equiv \sum_i \mathbf{p}_i$ is the total electronic momentum (with \mathbf{p}_i the electron momentum). Further progress is achieved by using the cumulant expansion method in Eq. (21.b). For dispersionless LO phonons (Einstein model) of frequency ω_0 , Eq. (21.b) can be approximated by the expression (Cheche and Chang, 2005)

$$\alpha(\omega) = \frac{2\pi e^2}{ncm_0^2 \hbar \omega V_0} \sum_{p, s \neq 0} \left[P_{0p} P_{s0} \int_{-\infty}^{\infty} dt \exp[i(\omega - \omega_p)t] \exp \left(-\sum_{i \neq 0} G_{piis} \right) \right], \quad (22)$$

where $G_{piis} \equiv g_{piis} \omega_0^2 I(t, p, i, i, s)$, $g_{kk'pp'} \equiv \sum_{\mathbf{q}} [M_{\mathbf{q}}^{kk'} M_{-\mathbf{q}}^{pp'} / (\hbar \omega_0)^2]$, ($g_{pppp} \equiv g_p$ is the Huang-Rhys factor), $I(t, k, k', k', p') = \int_0^t dt_1 \int_0^{t_1} dt_2 \exp(it_1 \omega_{kk'}) \exp(it_2 \omega_{k'p'}) D^0(t_1 - t_2)$, $D^0(t_1 - t_2) = [\bar{N} \exp(i\omega_0(t_1 - t_2)) + (\bar{N} + 1) \exp(-i\omega_0(t_1 - t_2))]$, $\bar{N} = 1/(e^{\beta \hbar \omega_0} - 1)$, and $\omega_{ij} = (E_i - E_j)/\hbar$.

If the off-diagonal coupling terms in Eq. (19) are disregarded then Eq. (22) is exact and it recovers the adiabatic limit (the Franck-Condon progression):

$$\alpha^{ad}(\omega) = \frac{4\pi^2 e^2}{ncm_0^2 \hbar \omega V_0} \sum_{f \neq 0} \left\{ |P_{0f}|^2 \exp[-g_f(2\bar{N} + 1)] \right. \\ \left. \times \sum_{n=-\infty}^{\infty} I_n \left(2g_f \sqrt{\bar{N}(\bar{N} + 1)} \right) \exp(n\beta \hbar \omega_0 / 2) \delta(\omega - \omega_f + \Delta_{ad}^f - n\omega_0) \right\} \quad (23)$$

where I_n are the modified Bessel functions, and $\Delta_{ad}^f = \omega_0 \sum_{\mathbf{q}} \left(|M_{\mathbf{q}}^{ff}|^2 \hbar^{-2} \omega_0^{-2} \right) \equiv \omega_0 g_f$ is the self-energy. The relative intensity of absorption lines is given by the coefficients of the Dirac delta functions.

Next, we adopt the spherical model from section 3.1.1 for spherical GaAs microcrystallites embedded in AlAs matrix. The quantity $P_{0f} P_{f'0} = |\mathbf{p}_{cv}^0|^2 3^{-1} A_{n_e n_h} A_{n_e' n_h'} \delta_{m_e m_h} \delta_{m_e' m_h'}$ in Eq. (21.b) is obtained by averaging over all space polarization directions. The Fröhlich coupling is written for dispersionless bulk LO phonons (for a spherical QD the interface modes do not couple with the exciton states (Melnikov & Fowler, 2002)). Within the pure-EHP approximation the EHP-phonon interaction reads (Voigt et. al., 1979; Nomura & Kobayashi, 1992)

$M_{\mathbf{q}}^{ff'} \rightarrow M_{\mathbf{q}}^{ab;a'b'} = V_0^{-1/2} f_0 q^{-1} \int d\mathbf{r}_e d\mathbf{r}_h \varphi_a^*(\mathbf{r}_e) \varphi_b^*(\mathbf{r}_h) \varphi_{a'}(\mathbf{r}_e) \varphi_{b'}(\mathbf{r}_h) [\exp(i\mathbf{q}\mathbf{r}_e) - \exp(i\mathbf{q}\mathbf{r}_h)]$, where f_0 is the Fröhlich coupling constant. Explicit expression of $M_{\mathbf{q}}^{ff'}$ for spherical QDs can be found in (Cheche and Chang, 2005).

For the only two optical levels which appear at $R_0 = 20$ (see Fig. 3), with an inter-level energy of approximately $11\hbar\omega_0$, the plot of absorption spectrum centred on the line A_0 obtained from Eq. (22) and that given by the adiabatic expression, Eq. (23) are, as expected, practically identical. Situation is different for $R_0 = 32 \text{ \AA}$, where the dark level D_1 is located between two optical levels A_0 and D_0 (see Fig. 3). Contribution of the optical and dark levels to the absorption centered on line A_0 is included in the following expression:

$$\alpha_1(\omega) = \frac{2\pi e^2 |\mathbf{p}_{cv}^0|^2}{3ncm_0^2 \hbar \omega V_0} A_{110}^2 \exp(-\Lambda_1) \sum_{p=-\infty}^{\infty} \sum_{k,r=0}^{\infty} \sum_{s,t=0}^{\infty} \left[I_p \left(2g_1 \sqrt{\bar{N}(\bar{N}+1)} \right) \right. \\ \times \left(\frac{\bar{N}g_{1221}\bar{\beta}^2}{k!} \right)^k \left(\frac{(\bar{N}+1)g_{1221}\bar{\gamma}^2}{r!} \right)^r \left(\frac{\bar{N}g_{1331}\bar{\beta}^2}{s!} \right)^s \left(\frac{(\bar{N}+1)g_{1331}\bar{\gamma}^2}{t!} \right)^t \exp\left(\frac{-p\hbar\omega_0}{2k_B T} \right) \\ \left. \times \delta[\omega - \omega_1 + \Delta_1 + p\omega_0 - k(\omega_{21} - \omega_0) - r(\omega_{21} + \omega_0) - s(\omega_{31} - \omega_0) - t(\omega_{31} + \omega_0)] \right] \quad (24)$$

with $\bar{\beta} \equiv \omega_0 / (\omega_{31} - \omega_0)$ and $\bar{\gamma} \equiv \omega_0 / (\omega_{31} + \omega_0)$. The non-adiabaticity effect expressed by Eq. (24) is shown in Fig. 5, where the absorption spectra at different temperatures are plotted (we dressed the lines by Lorentzians with a finite width of 15meV to simulate the EHP-acoustic phonons interaction). The adiabatic spectrum obtained with Eq. (23) has no temperature-induced shift and its maxima are not significantly changed with temperature. The following quantities obtained within the adopted QD model have been used: $E_1 = 1.8822\text{eV}$, $E_2 = 2.0738\text{eV}$, $E_3 = 1.9496\text{eV}$, $g_1 = 0.039$, $g_{1221} = 0.234$, and $g_{1331} = 0.904$. The stronger accompanying resonances are marked by arrows. The energy of some resonances are indicated by factors which multiply the LO phonon energy; they are placed to the left of the lines or arrows. The temperature dependence of the spectra, weak in the case of adiabatic treatment, becomes important now. Thus, decrease of intensity (by 37%) and red shift (from 1.87eV to 1.85eV) of the 0PL lines are obtained when temperature increases from 10K to 300K. This agrees with the behavior observed experimentally for CdTe QDs (Besombes et. al., 2001). On the other hand, the simulated Huang-Rhys factors reach values larger by two orders of magnitude than those of the bulk phase (0.0079 obtained from (Nomura & Kobayashi, 1992)). A similar behavior is reported for small self-assembled InAs/GaAs QDs by (García-Cristobal et. al. 1999). Thus, by the non-adiabatic activated channel at +0.86LO, the simulated Huang-Rhys factor obtained as the ratio of the line intensities for this accompanying resonance increases from 0.084 at $T = 10\text{K}$ to 0.23 at $T = 200\text{K}$. On the other hand, the non-adiabaticity effect manifests by strong resonances at 2.9LO (see Fig. 5), close to the third LO phonon replica as reported by some experiments, see, e.g., (Heitz et. al., 1997). The usual Franck-Condon progression is obtained by the adiabatic treatment (see the dotted line in Fig. 5).

Concluding this section, the non-adiabatic treatment presented, in accordance with the experimental observation, predicts: (i) accompanying resonances to the LO phonon satellites

in the optical spectra of QDs; (ii) red shift of the 0LO phonon lines and increased intensities of the accompanying resonances with temperature in the absorption spectra of QDs.

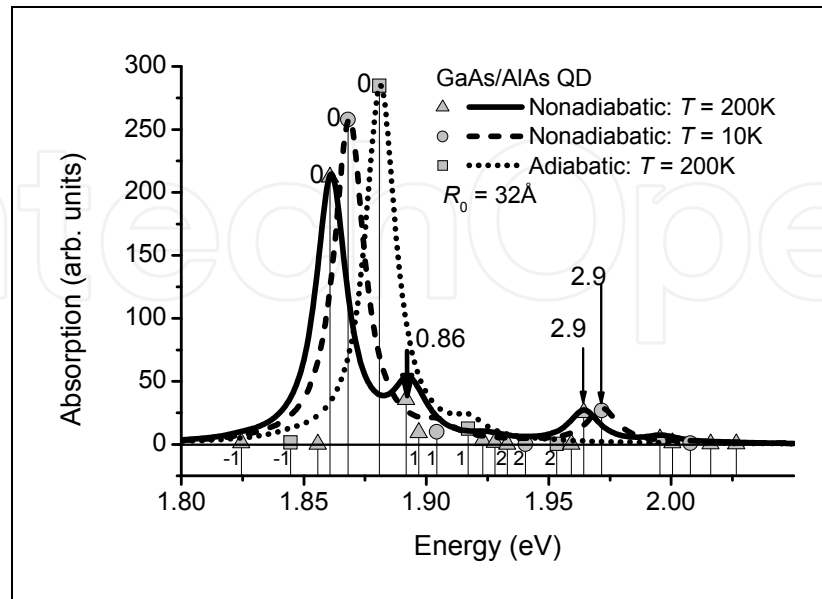


Fig. 5. Simulated absorption spectra of GaAs/AlAs nanocrystal QDs.

3.4 Phonon effect on the exciton and biexciton binding energy in cylindrical semiconductor quantum dots

In this section we discuss the exciton and biexciton emission spectra of polar semiconductor QDs within an adiabatic approach by using the configurational interaction method introduced in section 3.1.2. By taking into account the Fröhlich coupling between bi/exciton complexes and LO phonons, we simulate the *resonantly excited PL* spectrum (laser energy = detection energy + $n \cdot \text{LO energy}$, with n non-negative integer, (Sénès *et al.* 2005)) with linearly polarized (LP) light of InAs/AlAs cylindrical QDs. The exciton and biexciton binding energy for such QDs is also evaluated. In accordance with Eq. (9), we consider the following (multi)exciton-phonon Hamiltonian:

$$H^{(m)} = \sum_f \varepsilon_f^{(m)} X_f^{m+} X_f^m + \sum_{\mathbf{q}} \hbar \omega_0 b_{\mathbf{q}}^+ b_{\mathbf{q}} + \sum_{\mathbf{q}, f} M_{\mathbf{q}f}^{(m)} X_f^{m+} X_f^m (b_{\mathbf{q}} + b_{-\mathbf{q}}^+) = H_{\text{QD}}^{(m)} + H_{\text{ph}} + H_{\text{QD-ph}}^{(m)} \quad (25)$$

where $m = 1$ for exciton, $m = 2$ for biexciton, $b_{\mathbf{q}}^+$ ($b_{\mathbf{q}}$) are the bosonic creation (annihilation) operators of the phonons of mode \mathbf{q} , $M_{\mathbf{q}f}^{(m)}$ is the Fröhlich coupling, $M_{\mathbf{q}f}^{(m)} = \langle X_f^m | M_{(m)\mathbf{q}} | X_f^m \rangle$ and $M_{\mathbf{q}f}^{(m)} = M_{-\mathbf{q}f}^{(m)*}$ (from Hermiticity of $H^{(m)}$), ω_0 is the frequency of the dispersionless LO phonons, and $\sum_f \varepsilon_f^{(m)} X_f^{m+} X_f^m$ is the (multi)exciton H_D from Eq. (13) written in the language of (multi)exciton complexes. According to discussion from section 3.1.3, the Fröhlich electron-bulk LO phonon coupling is an acceptable approach for QD with high geometrical symmetry, where the interface modes are usually weak. Thus, for the exciton-LO phonon coupling (Voigt *et al.*, 1979; Nomura & Kobayashi, 1992)

$$M_{\mathbf{q}f}^{(1)} = \frac{f_0}{q\sqrt{V_0}} \langle X_f^1 | e^{i\mathbf{q}\cdot\mathbf{R}_e} - e^{i\mathbf{q}\cdot\mathbf{R}_h} | X_f^1 \rangle = \frac{f_0}{q\sqrt{V_0}} \sum |C_{\alpha\sigma,\beta\tau}^f|^2 \left[\langle \varphi_\alpha | e^{i\mathbf{q}\cdot\mathbf{R}} | \varphi_\alpha \rangle - \langle \varphi_\beta | e^{i\mathbf{q}\cdot\mathbf{R}} | \varphi_\beta \rangle \right], \quad (26)$$

and for biexciton-LO phonon coupling (Peter et. al., 2004)

$$M_{\mathbf{q}f}^{(2)} = \frac{f_0}{q\sqrt{V_0}} \langle X_f^2 | e^{i\mathbf{q}\cdot\mathbf{R}_{e1}} + e^{i\mathbf{q}\cdot\mathbf{R}_{e2}} - e^{i\mathbf{q}\cdot\mathbf{R}_{h1}} - e^{i\mathbf{q}\cdot\mathbf{R}_{h2}} | X_f^2 \rangle = \frac{f_0}{q\sqrt{V_0}} \sum_{\substack{\alpha_1\sigma_1,\alpha_2\sigma_2, \\ \beta_1\tau_1,\beta_2\tau_2}} |C_{\alpha_1\sigma_1,\alpha_2\sigma_2, \\ \beta_1\tau_1,\beta_2\tau_2}^f|^2 \quad (27)$$

$$\times \left[\langle \varphi_{\alpha_1} | e^{i\mathbf{q}\cdot\mathbf{R}} | \varphi_{\alpha_1} \rangle + \langle \varphi_{\alpha_2} | e^{i\mathbf{q}\cdot\mathbf{R}} | \varphi_{\alpha_2} \rangle - \langle \varphi_{\beta_1} | e^{i\mathbf{q}\cdot\mathbf{R}} | \varphi_{\beta_1} \rangle - \langle \varphi_{\beta_2} | e^{i\mathbf{q}\cdot\mathbf{R}} | \varphi_{\beta_2} \rangle \right]$$

where $f_0 = \sqrt{2\pi\hbar\omega_0} \mathbf{e}^2 (\varepsilon_\infty^{-1} - \varepsilon_0^{-1})$ is the Fröhlich coupling constant, and V_0 is the QD volume.

The emission spectrum of *single* QD corresponding to exciton and biexciton-exciton recombinations is obtained with the Fermi Golden Rule, that should be adapted to the composed system, multi(exciton)+phonons. The statistical operator $e^{-\beta H^{(m)}} / \text{Tr} \{ e^{-\beta H^{(m)}} \}$ is used for the statistical average in the Kubo formula of the optical conductivity. When applying the Fermi Golden Rule for the system multi(exciton)+phonons, we need to consider a *statistical* average for phonons and a *quantum* average for the *finite* number of multi(exciton) states in the QD. On the other hand, within the adiabatic approximation, the electronic potential energy surface is the potential for phonons in the QD. We imaginarily decompose temporally the absorption process and consider that before switching on the electron-phonon interaction, the electron-hole potential energy surface is raised vertically from the lowest potential energy surface of the exciton vacuum state to the excited potential energy surface (see dotted line parabola in Fig. 6). Then, we consider the electron-phonon interaction is switched on and as a result the potential energy surface is further modified to the new potential energy surface of the interacting multi(exciton)+phonon system, see upper solid line parabola in Fig. 6 and comments in (Odnoblyudov et. al., 1999).

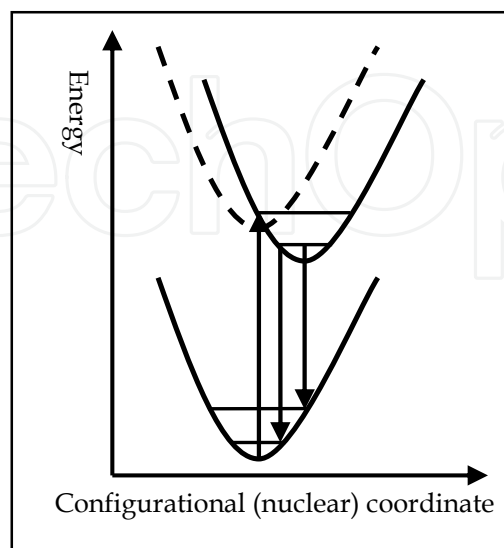


Fig. 6. Schematic exciton of the potential energy surface involved in transition.

Thus, according to its PES, each (multi)exciton state is characterized by its density matrix. To take into account the above considerations, we project the statistical operator of the phonon system interacting with the (multi)exciton state on the state $|X_i^m\rangle$ and write $\rho_i^{(m)} = \exp[-\beta(H_{ph} + h_i^{(m)})]/Z_i^{(m)}$, with $Z_i^{(m)} = \text{Tr}\langle X_i^m | \exp[-\beta(H_{ph} + H_{QD-ph}^{(m)})] | X_i^m \rangle$, and $h_i^{(m)} = \sum_{\mathbf{q}} M_i^{(m)}(b_{\mathbf{q}} + b_{-\mathbf{q}}^+)$. The partition function $Z_i^{(m)} = \prod_{\mathbf{q}} Z_{i\mathbf{q}}^{(m)}$ is the product of the partition functions for each mode having the wave vector \mathbf{q} . By dropping all \mathbf{q} subscripts, the partition function for a single mode reads, $Z_i^{(m)} = \text{Tr}\left\{\exp\left[-\beta\left(\hbar\omega_0 b^+ b + M_i^{(m)}(b + b^+)\right)\right]\right\}$. It can be evaluated by using a canonical transformation

$$Z_i^{(m)} = \text{Tr}\left\{\exp(S_i^{(m)})\exp\left[-\beta\left(\hbar\omega_0 b^+ b + M_i^{(m)}(b + b^+)\right)\right]\exp(-S_i^{(m)})\right\} \tag{28.a}$$

where the anti-Hermitian operator is defined as $S_i^{(m)} = (M_i^{(m)*} b^+ - M_i^{(m)} b)/(\hbar\omega_0)$. With $\exp[S_i^{(m)}] b^+ \exp[-S_i^{(m)}] = b^+ - M_i^{(m)}/\hbar\omega_0$, $\exp[S_i^{(m)}] b \exp[-S_i^{(m)}] = b - M_i^{(m)}/\hbar\omega_0$ one obtains $Z_i^{(m)} = \text{Tr}\left\{\exp\left[-\beta\left[\hbar\omega_0 b^+ b + (\hbar\omega_0)^{-1} |M_i^{(m)}|^2\right]\right]\right\} = (1 - \exp(-\beta\hbar\omega_0))^{-1} \exp\left[-\beta(\hbar\omega_0)^{-1} |M_i^{(m)}|^2\right]$, and

$$Z_i^{(m)} = \exp(-\beta\hbar\omega_0 g_i^{(m)}) \prod_{\mathbf{q}} (1 - e^{-\beta\hbar\omega_0})^{-1} \tag{28.b}$$

in which $g_i^{(m)} = \sum_{\mathbf{q}} |M_{\mathbf{q}i}^{(m)}|^2 / (\hbar^2 \omega_0^2)$ is the Huang-Rhys factor.

With the Fermi Golden Rule, the exciton emission spectrum is given by

$$\begin{aligned} I_X(\omega) &= \frac{2\pi}{\hbar} \sum_{\Gamma} A_{\nu\Gamma}^{(1)} \sum_{\mathbf{G}} |W_{\mathbf{G}\Gamma}|^2 \delta(\hbar\omega + E_{\mathbf{G}} - E_{\Gamma}) = \frac{1}{\hbar^2} \int_{-\infty}^{\infty} dt e^{i\omega t} \\ &\times \sum_{\Gamma} A_{\nu\Gamma}^{(1)} \langle X_{i\nu}^1 | e^{-itH^{(1)}/\hbar} H_{X^1-R} \left(\sum_{j,\mu} \left(|X_{j\mu}^1\rangle\langle X_{j\mu}^1| \right) + |\mathbf{G}\rangle\langle\mathbf{G}| \right) e^{itH_{ph}/\hbar} H_{X^1-R} | X_{i\nu}^1 \rangle \\ &= \frac{1}{\hbar^2} \int_{-\infty}^{\infty} dt e^{i\omega t} \sum_{\nu,i} \langle \nu | \rho_i^{(1)} | \nu \rangle \langle X_i^1 | e^{-itH^{(1)}/\hbar} H_{X^1-R} e^{itH_{ph}/\hbar} H_{X^1-R} | X_i^1 \rangle | \nu \rangle \\ &= \frac{1}{\hbar^2} \int_{-\infty}^{\infty} dt e^{i\omega t} \sum_i \text{Tr} \left\{ \langle X_i^1 | e^{-\beta(H_{ph} + h_i^{(1)})/\hbar} Z_i^{(1)-1} e^{-itH^{(1)}/\hbar} H_{X^1-R} e^{itH_{ph}/\hbar} H_{X^1-R} | X_i^1 \rangle \right\} \end{aligned} \tag{29}$$

where $|X_{i\nu}^1\rangle \equiv |X_i^1\rangle | \nu \rangle$ is the initial state with energy E_{Γ} and $|\mathbf{G}\rangle$ is the ground state with energy $E_{\mathbf{G}}$. H_{X^1-R} does not couple the exciton-phonon states, that is relation $\langle X_{in}^1 | H_{X^1-R} | X_{jn}^1 \rangle = 0$ holds, and in Eq. (29) we inserted $\sum_{j,\mu} \left(|X_{j\mu}^1\rangle\langle X_{j\mu}^1| \right)$ to make use of the

closure relation $\sum_{j,\mu} (|X_{j\mu}^1\rangle\langle X_{j\mu}^1|) + |G\rangle\langle G| = \mathbf{1}$. Since $[H_{QD}^{(1)}, H_{ph} + H_{QD-ph}^{(1)}] = 0$, by using the operator relation $e^{A+B} = e^A e^B e^{-[A,B]/2}$, we have

$$\langle X_i^1 | e^{-itH^{(1)}/\hbar} = \langle X_i^1 | e^{-itH_{QD}^{(1)}/\hbar} e^{-it(H_{ph} + H_{QD-ph}^{(1)})/\hbar} = e^{-it\varepsilon_i^{(1)}/\hbar} e^{-it(h_i^{(1)} + H_{ph})/\hbar} \langle X_i^1 |, \quad (30.a)$$

and

$$H_{X^1-R} H_{X^1-R} |X_i^1\rangle = \omega^{-2} \sum_i |C^i|^2 |X_i^1\rangle, \quad (30.b)$$

With Eqs. (30.a, b), Eq. (29) reads

$$I_X(\omega) = \frac{1}{\hbar^2} \int_{-\infty}^{\infty} dt e^{i\omega t} e^{-it\varepsilon_i^{(1)}/\hbar} \sum_i |C^i|^2 F_{1ph}^{(i)}(t) \quad (31)$$

where the correlation function is

$$F_{1ph}^{(i)}(t) = Tr \left\{ e^{-\beta(h_i^{(1)} + H_{ph})/\hbar} Z_i^{(1)-1} e^{-it(h_i^{(1)} + H_{ph})/\hbar} e^{itH_{ph}/\hbar} \right\}. \quad (32.a)$$

Eq. (32.a) is transformed by using the canonical transformation,

$$\begin{aligned} F_{1ph}^{(i)}(t) &= Tr \left\{ e^{S_i^{(1)}} e^{-\beta(h_i^{(1)} + H_{ph})/\hbar} Z_i^{(1)-1} e^{-S_i^{(1)}} e^{S_i^{(1)}} e^{-it(h_i^{(1)} + H_{ph})/\hbar} e^{-S_i^{(1)}} e^{S_i^{(1)}} e^{itH_{ph}/\hbar} e^{-S_i^{(1)}} \right\} \\ &= Tr \left\{ e^{-\beta(\bar{h}_i^{(1)} + \bar{H}_{ph})/\hbar} Z_i^{(1)-1} e^{-it(\bar{h}_i^{(1)} + \bar{H}_{ph})/\hbar} e^{it\bar{H}_{ph}/\hbar} \right\} \end{aligned} \quad (32.b)$$

where, generally ($m = 1, 2$),

$$S_i^{(m)} = \frac{1}{\hbar\omega_0} \sum_{\mathbf{q}} M_{i\mathbf{q}}^{(m)} (b_{-\mathbf{q}}^+ - b_{\mathbf{q}}), \quad (32.c)$$

and $\bar{H}_{ph} + \bar{h}_i^{(1)} = H_{ph} - \hbar g_i^{(1)} \omega_0$, $\bar{H}_{ph} = H_{ph} - h_i^{(1)} + \hbar g_i^{(1)} \omega_0$. With these two last equalities substituted in Eq. (32.b) we write

$$\begin{aligned} F_{ph}^{(i)}(t) &= e^{2ig_i^{(1)}\omega_0 t} Tr \left\{ e^{-\beta H_{ph}/\hbar} Z_{ph}^{-1} e^{-itH_{ph}/\hbar} e^{it(H_{ph} - h_i^{(1)})/\hbar} \right\} = e^{2ig_i^{(1)}\omega_0 t} Tr \left\{ \rho e^{-itH_{ph}/\hbar} e^{it(H_{ph} - h_i^{(1)})/\hbar} \right\}, \\ &= e^{2ig_i^{(1)}\omega_0 t} \left\langle e^{-itH_{ph}/\hbar} e^{it(H_{ph} - h_i^{(1)})/\hbar} \right\rangle_0 \equiv e^{2ig_i^{(1)}\omega_0 t} \left\langle U_{ph}^{(i)}(t) \right\rangle_0 \end{aligned} \quad (32.d)$$

where Z_{ph} is the partition function of the phonon system. By using the interaction representation, the correlation function reads

$$\left\langle U_{ph}^{(i)}(t) \right\rangle_0 = T \left\langle \exp \left[-i \int_0^t dt_1 \tilde{h}_i^{(1)}(t_1) \right] \right\rangle_0 \quad (33.a)$$

where T is the time-ordering operator and

$$\tilde{h}_i^{(1)}(t) = e^{-iH_{ph}/\hbar} \left(h_i^{(1)} / \hbar \right) e^{iH_{ph}/\hbar} = \sum_{\mathbf{q}} \frac{M_{\mathbf{q}i}^{(1)}}{\hbar} \left(b_{\mathbf{q}} e^{i\omega_0 t} + b_{-\mathbf{q}}^+ e^{-i\omega_0 t} \right) \quad (33.b)$$

Next, to evaluate $\langle U_{ph}^{(i)}(t) \rangle_0$ we use the linked cluster expansion (Mahan, 2000)

$$\langle U_{ph}^{(i)}(t) \rangle_0 = \sum (-i)^n \langle U_n^{(i)}(t) \rangle_0, \quad \langle U_n^{(i)}(t) \rangle_0 = \frac{1}{n!} \int_0^t dt_1 \int_0^{t_1} dt_2 \dots \int_0^{t_{n-1}} dt_n \langle T \tilde{h}_i^{(1)}(t_1) \dots \tilde{h}_i^{(1)}(t_n) \rangle_0 \quad (33.c)$$

and since $\tilde{h}_i^{(1)}$ describes creation or annihilation of a phonon, they are grouped in pairs. Thus,

$$\begin{aligned} \langle U_0^{(i)}(t) \rangle_0 &= 1, \quad \langle U_1^{(i)}(t) \rangle_0 = 0, \\ \langle U_2^{(i)}(t) \rangle_0 &= \frac{1}{2\hbar^2} \int_0^t dt_1 \int_0^{t_1} dt_2 \sum_{\mathbf{q}} |M_{\mathbf{q}i}^{(1)}|^2 \left[(1 + \bar{N}) e^{i\omega_0 |t_1 - t_2|} + \bar{N} e^{-i\omega_0 |t_1 - t_2|} \right] \\ &= \sum_{\mathbf{q}} \frac{2g_i^{(1)}}{2} \left[(1 + \bar{N})(1 - e^{i\omega_0 t}) + \bar{N}(1 - e^{-i\omega_0 t}) + i\omega_0 t \right] = \sum_{\mathbf{q}} \frac{\phi_{\mathbf{q}i}^{(1)}(t)}{2} \end{aligned} \quad (33.d)$$

By using Wick's theorem to pair the boson operators for the terms of higher order one obtains (Mahan, 2000)

$$\langle U_{2m}^{(i)}(t) \rangle_0 = \frac{1}{m!} \left[\sum_{\mathbf{q}} \frac{\phi_{\mathbf{q}i}^{(1)}(t)}{2} \right]^m \quad (33.e)$$

and, consequently

$$\begin{aligned} \langle U_{ph}^{(i)}(t) \rangle_0 &= \sum_{m=0}^{\infty} (-1)^m \langle U_{2m}^{(i)}(t) \rangle_0 = \exp \left[- \sum_{\mathbf{q}} \frac{\phi_{\mathbf{q}i}^{(1)}(t)}{2} \right] \\ &= \exp \left\{ -g_i^{(1)} \left[2\bar{N} + 1 - 2\sqrt{\bar{N}(\bar{N} + 1)} \cos[\omega_0(t + i\beta\hbar/2) + i\omega_0 t] \right] \right\} \\ &= e^{-g_i^{(1)}(2\bar{N} + 1)} \sum_{l=-\infty}^{\infty} I_l \left[2g_i^{(1)} \sqrt{\bar{N}(\bar{N} + 1)} \right] e^{l\beta\hbar\omega_0/2} e^{il\omega_0 t} e^{-ig_i^{(1)}\omega_0 t} \end{aligned} \quad (33.f)$$

With Eqs. (32.d) and (33.f), Eq. (29) that gives the exciton emission spectrum reads

$$I_X(\omega) = \frac{2\pi}{\hbar^2 \omega^2} \sum_i |\mathbf{C}^i|^2 e^{-g_i^{(1)}(2\bar{N} + 1)} \sum_{l=-\infty}^{\infty} I_l \left[2g_i^{(1)} \sqrt{\bar{N}(\bar{N} + 1)} \right] e^{l\beta\hbar\omega_0/2} \delta \left[\omega - \varepsilon_i^{(1)} / \hbar + (g_i^{(1)} + l)\omega_0 \right] \quad (34)$$

where \mathbf{C}^i is defined in Eq. (17.a). I_l is the modified Bessel function obtained from expansion in Eq. (33.f), $\exp[z \cos \theta] = \sum_{l=-\infty}^{\infty} I_l(z) \exp(il\theta)$. Eq. (34) shows the usual phonon

progression and comparatively to Eq. (23) in the argument of the Dirac delta function the sign of factor for the phonon progression is changed.

With the Fermi Golden Rule, the biexciton-exciton emission spectrum is given by

$$\begin{aligned}
 I_{XX}(\omega) &= \frac{2\pi}{\hbar} \sum_{\Gamma} A v_{\Gamma}^{(2)} \sum_{\Gamma} |W_{\Gamma}|^2 \delta(\hbar\omega + E_{\Gamma} - E_i) = \frac{1}{\hbar^2} \int_{-\infty}^{\infty} dt e^{i\omega t} \sum_{\Gamma} A v_{\Gamma}^{(2)} \langle X_{i\nu}^2 | e^{-itH^{(2)}/\hbar} H_{X^2-R} \\
 &\times \left(\sum_{f,\mu} |X_{f\mu}^2\rangle \langle X_{f\mu}^2| + |G\rangle \langle G| + |X_{f\mu}^1\rangle \langle X_{f\mu}^1| \right) e^{itH^{(1)}/\hbar} H_{X^2-R} |X_{i\nu}^2\rangle \\
 &= \frac{1}{\hbar^2} \int_{-\infty}^{\infty} dt e^{i\omega t} \sum_{\nu,i} \langle \nu | \rho_i^{(2)} | \nu \rangle \langle \nu | \langle X_i^2 | e^{-itH^{(2)}/\hbar} H_{X^2-R} e^{itH^{(1)}/\hbar} H_{X^2-R} | X_i^2 \rangle | \nu \rangle \\
 &\equiv \frac{1}{\hbar^2 Z^{(2)}} \int_{-\infty}^{\infty} dt e^{i\omega t} \sum_i \text{Tr} \left\{ \langle X_i^2 | e^{-\beta(H_{ph} + h_i^{(2)})/\hbar} e^{-itH^{(2)}/\hbar} H_{X^2-R} e^{itH^{(1)}/\hbar} H_{X^2-R} | X_i^2 \rangle \right\}
 \end{aligned} \tag{35}$$

where $|X_{i\nu}^2\rangle \equiv |X_i^2\rangle | \nu \rangle$ is the biexciton initial state with energy E_i , and $|X_{f\nu}^1\rangle \equiv |X_f^1\rangle | \nu \rangle$ is the exciton final state with energy E_f . H_{X^2-R} does not couple the biexciton-phonon states and the ground state to the biexciton-phonon states, that is the relations $\langle X_{i\nu}^2 | H_{X^2-R} | X_{j\mu}^2 \rangle = 0$ and $\langle X_{i\nu}^2 | H_{X^2-R} | 0 \rangle | \mu \rangle = 0$ hold, and in Eq. (35) we inserted

$|G\rangle \langle G| + \sum_{f,\mu} |X_{f\mu}^2\rangle \langle X_{f\mu}^2|$ to make use of the closure relation, $\sum_{f,\mu} (|X_{f\mu}^2\rangle \langle X_{f\mu}^2| + |X_{f\mu}^1\rangle \langle X_{f\mu}^1|) + |G\rangle \langle G| = \mathbf{1}$. Similarly to Eq. (30.a) we have $\langle X_i^2 | e^{-itH^{(2)}/\hbar} = e^{-it\varepsilon_i^{(2)}/\hbar} e^{-it(h_i^{(2)} + H_{ph})/\hbar} \langle X_i^1 |$. Next, Eq. (17.b) is inserted for H_{X^2-R} in Eq. (35). From the four terms containing four (multi)exciton operators involved by this substitution, only one has non-zero contribution and

$$\begin{aligned}
 &\langle X_i^2 | e^{-\beta(H_{ph} + h_i^{(2)})/\hbar} e^{-itH^{(2)}/\hbar} H_{X^2-R} e^{itH^{(1)}/\hbar} H_{X^2-R} | X_i^2 \rangle \\
 &= \omega^{-2} \sum_{a,b,c,d} C^{ab} C^{cd*} \langle X_i^2 | e^{-\beta(H_{ph} + h_i^{(2)})/\hbar} e^{-itH^{(2)}/\hbar} X_a^{2+} X_b^1 e^{itH^{(1)}/\hbar} X_c^{1+} X_d^2 | X_i^2 \rangle
 \end{aligned}$$

With additional algebra and making use of $X_a^{2+} X_b^1 = |X_a^2\rangle \langle X_b^1|$, one obtains

$$\begin{aligned}
 &\langle X_i^2 | e^{-\beta(H_{ph} + h_i^{(2)})/\hbar} e^{-itH^{(2)}/\hbar} H_{X^2-R} e^{itH^{(1)}/\hbar} H_{X^2-R} | X_i^2 \rangle \\
 &= \omega^{-2} \sum_f |C^{if}|^2 e^{-it(\varepsilon_i^{(2)} - \varepsilon_f^{(1)})/\hbar} e^{-\beta(H_{ph} + h_i^{(2)})/\hbar} e^{-it(H_{ph} + h_i^{(2)})/\hbar} e^{it(H_{ph} + h_f^{(1)})/\hbar}
 \end{aligned} \tag{36}$$

With Eqs. (36), Eq. (35) reads

$$I_{XX}(\omega) = \frac{1}{\hbar^2 \omega^2} \int_{-\infty}^{\infty} dt e^{i\omega t} \sum_{i,f} |C^{if}|^2 e^{-it(\varepsilon_i^{(2)} - \varepsilon_f^{(1)})/\hbar} F_{2ph}^{(if)}(t) \tag{37}$$

where the correlation function is

$$F_{2ph}^{(if)}(t) = Tr \left\{ e^{-\beta H_{0i}/\hbar} Z_i^{(2)-1} e^{-itH_{0i}/\hbar} e^{it(H_{0i}+V_{if})/\hbar} \right\} \tag{38.a}$$

with $H_{0i} = H_{ph} + h_i^{(2)}$, $H_{ph} + h_f^{(1)} = H_{0i} + h_f^{(1)} - h_i^{(2)} = H_{0i} + V_{if}$, and $Z_i^{(2)}$ is defined by Eq. (28.b). $F_{2ph}^{(if)}(t)$ is evaluated by the same procedure of the canonical transformation used for $F_{1ph}^{(i)}(t)$. Thus, in Eq. (38.a) one inserts the unitary operator $e^{-S_i^{(2)}} e^{S_i^{(2)}}$, with $S_i^{(2)}$ defined by Eq. (32.c) and one obtains

$$F_{2ph}^{(if)}(t) = Tr \left\{ e^{-\beta \bar{H}_{0i}/\hbar} Z_i^{(2)-1} e^{-it\bar{H}_{0i}/\hbar} e^{it(\bar{H}_{0i}+\bar{V}_{if})/\hbar} \right\} \tag{38.b}$$

with $\bar{H}_{0i} = H_{ph} - \hbar g_i^{(2)} \omega_0$, $\bar{H}_{0i} + \bar{V}_{if} = H_{ph} + h_{if} + \hbar \omega_0 (g_{if} - g_b^{(1)})$, $h_{if} = \sum_{\mathbf{q}} [(M_{\mathbf{q}f}^{(1)} - M_{\mathbf{q}i}^{(2)}) \times (b_{\mathbf{q}} + b_{-\mathbf{q}}^+)]$, and $g_{if} = (\hbar \omega_0)^{-2} \sum_{\mathbf{q}} |M_{\mathbf{q}f}^{(1)} - M_{\mathbf{q}i}^{(2)}|^2$. With these quantities, we rewrite Eq. (38.b) as follows

$$\begin{aligned} F_{2ph}^{(if)}(t) &= e^{it[g_i^{(2)} - g_f^{(1)} + g_{if}]\omega_0} Tr \left\{ e^{-\beta H_{ph}/\hbar} Z_{ph}^{-1} e^{-itH_{ph}/\hbar} e^{it(H_{ph}+h_{if})/\hbar} \right\} \\ &= e^{it[g_i^{(2)} - g_f^{(1)} + g_{if}]\omega_0} Tr \left\{ \rho e^{-itH_{ph}/\hbar} e^{it(H_{ph}+h_{if})/\hbar} \right\} \\ &\equiv e^{it[g_i^{(2)} - g_f^{(1)} + g_{if}]\omega_0} \left\langle e^{-itH_{ph}/\hbar} e^{it(H_{ph}+h_{if})/\hbar} \right\rangle_0 \equiv e^{it[g_i^{(2)} - g_f^{(1)} + g_{if}]\omega_0} \left\langle U_{ph}^{(if)}(t) \right\rangle_0 \end{aligned} \tag{38.c}$$

Given the similarity between expressions of the correlation functions (see Eqs. (32.d) and (38.c)), we evaluate $\left\langle U_{ph}^{(if)}(t) \right\rangle_0$ by the same procedure used for evaluation of $\left\langle U_{ph}^{(i)}(t) \right\rangle_0$ and obtain

$$\begin{aligned} \left\langle U_{ph}^{(if)}(t) \right\rangle_0 &= \exp \left\{ - \sum_{\mathbf{q}} g \left[(1 + \bar{N}) (1 - e^{i\omega_0 t}) + \bar{N} (1 - e^{-i\omega_0 t}) + i\omega_0 t \right] \right\} \\ &= e^{-g_{if} (2\bar{N} + 1)} \sum_{l=-\infty}^{\infty} I_l \left[2g_{if} \sqrt{\bar{N}(\bar{N} + 1)} \right] e^{l\beta\hbar\omega_0/2} e^{il\omega_0 t} e^{-ig_{if}\omega_0 t} \end{aligned} \tag{38.d}$$

With Eqs. (38.c, d), Eq. (37) that gives the biexciton-exciton emission spectrum reads

$$\begin{aligned} I_{XX}(\omega) &= \frac{2\pi}{\hbar^2 \omega^2} \sum_{f,i} \left\{ \left(|C^{if}|^2 \exp[-g_{if} (2\bar{N} + 1)] \beta \hbar \omega_0 \right) \right. \\ &\quad \left. \times \sum_{l=-\infty}^{\infty} I_l \left[2g_{if} \sqrt{\bar{N}(\bar{N} + 1)} \right] \exp(l\beta\hbar\omega_0/2) \delta \left[\omega - (\varepsilon_i^{(2)} - \varepsilon_f^{(1)})/\hbar + (g_i^{(2)} - g_f^{(1)} + l)\omega_0 \right] \right\} \end{aligned} \tag{39}$$

with C^{if} defined by Eq. (17.b). g_{if} is function of the difference between the coupling of phonons to the initial biexciton $|X_i^2\rangle$ and the final exciton state, $|X_f^1\rangle$; it influences the

intensity of the emission line. Note that g_{if} cancels out from the argument of the Dirac delta function from Eq. (39), instead and a difference of the Huang Rhys factors, $g_i^{(2)} - g_f^{(1)}$, is present. Eq. (39) has similarity with Eq. (34), and all characteristics of an emission spectrum are present. The spectra have ω^{-2} dependence. In Eqs. (34) and (39) the argument of the modified Bessel functions, I_l , plays major role in establishing the emission line intensity; a larger Huang-Rhys factor will result in more intense lines.

Next, we apply the theory to the resonantly excited photoluminescence for high barrier heterostructure of InAs/AlAs. According to the model from section 3.1.2, the mixing of the bi/exciton states by phonons is absent, and the formula (34) and (39) are valid. On the other hand, the bi/exciton degeneracy could make the dynamical Jahn-Teller effect (Jahn & Teller, 1937) to be effective. Accordingly to Eq. (39), the coupling Huang-Rhys factor g_{if} makes the degenerate lines to have different intensities. We approximate the intensity of emission lines by an average over the intensity of degenerate levels. The values of Huang-Rhys factors obtained, in accordance with (García-Cristóbal et. al., 1999; Cheche et. al., 2005) are large as follows: $g_1^{(1)} = 0.187$, $g_2^{(1)} = 0.103$, $g_3^{(1)} = 0.104$, $g_1^{(2)} = 0.747$, $g_2^{(2)} = 0.364$, $g_3^{(2)} = 0.365$, $g_4^{(2)} = 0.364$, and the g_{if} have values between 0.103 and 0.187, and larger values of 0.704 for g_{12} , and 0.706 for g_{13} . According to the presence of the Huang-Rhys factor in the argument of the modified Bessel functions, I_l , from Eqs. (34) and (39), a large Huang-Rhys factors obtained may be the sign of the appearance of strong phonon replicas in the optical spectra.

There is a variety of results regarding the biexciton binding energy, which reveal importance of shape, compounds, and size of QDs. In Fig. 7 the biexciton binding ground state (GS) energy, the difference of biexciton and exciton GS lines as given by Eqs. (34) and (39), i.e., $\tilde{\varepsilon}_b^{2X-X} = 2\varepsilon_1^{(1)} - \varepsilon_1^{(2)} - (2g_1^{(1)} - g_1^{(2)})\hbar\omega_0$, is obtained for different values of $\hbar\omega_e$ (with $\omega_e/\omega_h = 3$). Results from Fig. 7 show that the biexciton binding energy increases when the in-plane parabolic potential increases (QD radius decreases or exciton GS energy increases). This result is in agreement with the experimental data obtained for the same cylindrical shape of QD but with other compounds, InAs/InP (Chauvin et. al., 2006)), $\text{In}_{0.14}\text{Ga}_{0.86}\text{As}/\text{GaAs}$ (Bayer et. al., 1998) or with theoretical results obtained for GaAs.

QDs (Ikezawa et. al., 1998). An opposite behavior is reported for InAs/GaAs truncated pyramidal QDs by (Rodt, 2005). These facts might be related with the actual shape of the QDs. On the other hand, the binding character is obtained for smaller QDs ($\hbar\omega_e$ of order of tens of meV) and the antibinding character for larger QDs (for example, with $\hbar\omega_e = 0.001$ eV, we obtain $\tilde{\varepsilon}_b^{2X-X} = -0.0011$ eV) in agreement with (Stier, 2001). Remarkable for the relevance of LO phonon influence on the spectra is the fact that without taking into account the self-energy (setting up $g_1^{(1)} = g_1^{(2)} = 0$ in Eq. (39)), $\varepsilon_b^{2X-X} = 2\varepsilon_1^{(1)} - \varepsilon_1^{(2)}$ is negative (increasing, e.g., from -0.0034 eV for $\hbar\omega_e = 0.065$ eV to -0.0008 eV for $\hbar\omega_e = 0.005$ eV) and $\tilde{\varepsilon}_b^{2X-X}$ becomes positive only by considering the phonon coupling.

These observations show that in addition to the shape, size, chemical composition, electron-hole exchange interaction, and piezoelectricity, the LO phonon coupling is an important factor which influences the anti/binding character of the biexciton. The extent to which the LO phonon coupling can not be neglected is a problem which can be addressed within a QD model of high enough accuracy. The confidence in the QD model we used is supported, in addition to the results obtained for biexciton, by those obtained for the exciton complex. As shown in Fig. 7, the magnitude of the exciton GS energy and decreasing of the exciton GS energy with QD size agree with other reports, see, e.g., (Ikezawa, 2006; Grundmann et. al., 1995). As the piezoelectricity in the case of cylindrical QD shape is expected to be less important (Miska, 2002) than for other QD shapes, the adopted QD model is suitable for describing the main physics of the bi/exciton-LO phonon coupling in cylindrical semiconductor QDs.

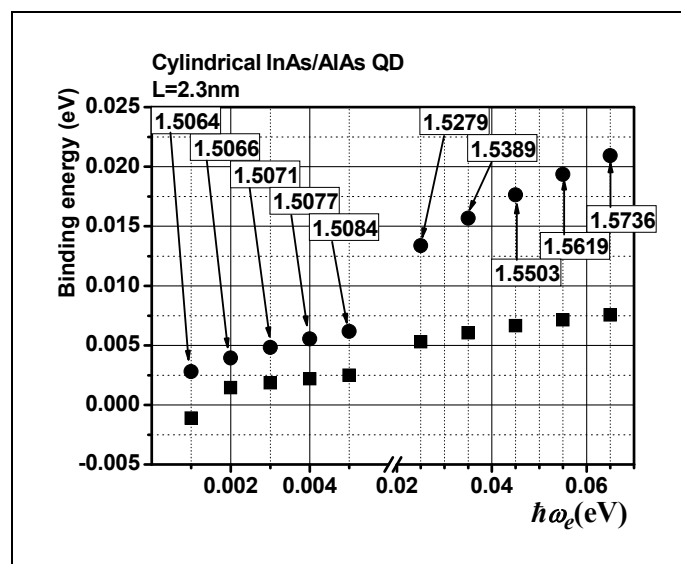


Fig. 7. The exciton (•) and biexciton (■) binding energies obtained for the simulated InAs/AlAs QD. The numbers show the energy of the exciton GS emission line.

The calculations show that value of exciton and biexciton binding energy is strongly influenced by diameter (in-plane confinement) and less by the height (perpendicular confinement) of cylindrical QDs. The binding character of the biexciton, with $\tilde{\varepsilon}_b^{2X-X} = 0.0076$ eV, and the exciton and biexciton GS emission lines of InAs/AlAs QD as reported by (Sarkar et. al., 2006) for $T = 9$ K are simulated in Fig. 8 by choosing $\hbar\omega_e = 0.065$ eV and $\hbar\omega_h = (0.065/3)$ eV. Regarding the emission, the emission lines from Fig. 8 are labeled with three digits for transition from biexciton state (first digit) to exciton state (second digit), and with two digits for transition from exciton state (first digit) to the VS (reminding to the reader, VS means vacuum state, that is, the no excitons state); the last digit corresponds to the phonon replica. The open squares show the experimental results from

(Sarkar, 2006). The inset shows schematically the exciton resonant emission we simulated. Emission spectra of InAs/AlAs QDs are reported in a range of 1.5-1.9eV (Dawson et. al. 2005; Offermans et. al., 2005; Sarkar et. al., 2006). Our approach simulates the emission from exciton (1, 0) GS and biexciton (1, 1, 0) GS, in the range 1.56-1.68eV. In this interval the phonon replicas are predicted in accordance with the experimental data from (Sarkar et. al., 2005).

The literature regarding the presence of the excited states in emission spectra of QDs is rather scarce (Kamada, 1998; Khatsevich, 2005). The strong LO emission lines from excited states might explain the higher energy lines observed in the PL spectra reported by (Dawson et. al. 2005; Offermans et. al., 2005; Sarkar et. al., 2005). For small enough InAs/AlAs QDs the lowest energy state at Γ point in InAs moves above the AlAs X band edge, the electrons spread in the AlAs barrier, and appearance of high energy lines by this mechanism is forbidden. Instead, the exciton line (2, 0) and the biexciton-exciton emission lines (3, 1, 0), and (2, 1, 0) are candidates for explaining the high energy lines observed by (Offermans et. al., 2005). Accuracy of our QD model is not high enough to explain the fine-structure splitting reported by (Sarkar et. al., 2006) and shown in Fig. 8; the fine-structure is assigned to the electron-hole exchange interaction, which was neglected in our model. Prediction for higher temperatures is not reliable, as far as the possible dissociation of the biexciton with temperature had not been taken into by the present considerations. However, at larger, but still low temperatures, under 60K, the features of spectra predicted by our approach do not change significantly.

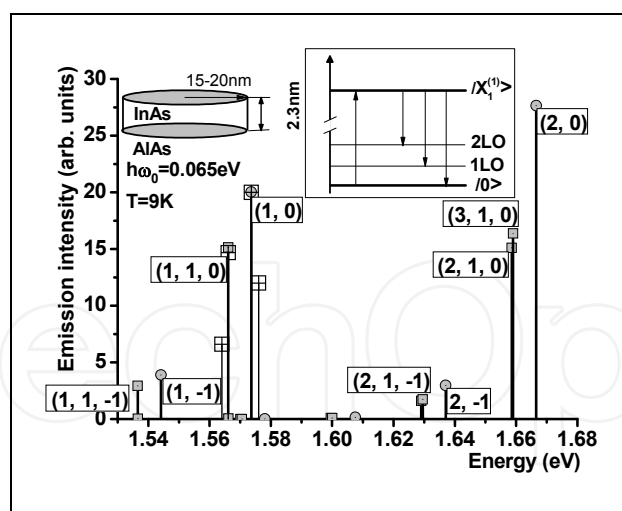


Fig. 8. The resonant emission spectrum of biexciton and exciton complexes.

Concluding this section, the theoretical approach we introduced is a useful tool for describing the influence of LO phonons on the resonant excitation emission at low temperatures. The high energy emission lines, that are obtained by configurational interaction calculations for cylindrical InAs/AlAs QDs, are associated to the emission from

the excited states. One finds, in accordance with the experiment, that the biexciton binding energy has a binding character (positive value), which diminishes with decreasing the radius of QD, and becomes antibinding (negative value) for flat QDs. The simulated exciton and biexciton binding energies obtained, demonstrate that the phonon coupling is an essential factor, which should be integrated in the analyses for an accurate description of optical transitions in QDs. For the InAs/AlAs QDs, the presence of LO phonon replicas and emission from the excited states is explained as the consequence of large Huang-Rhys factors.

4. Outlook

To introduce the reader the problem of the electron-phonon interaction in QDs, three basic aspects are presented in the Sec. 2: i) the adiabatic and non-adiabatic transitions in the optical transitions; ii) the Huang-Rhys factor; iii) the Hamiltonian of localized defect with several electronic states mixed by phonons.

In Sec. 3.1, within the effective mass approximation two models describing the electronic energy structure of spherical GaAs/AlAs QDs and cylindrical InAs/AlAs QDs are introduced. For the optical transitions, the spherical QD model predicts the adiabatic treatment is appropriate for QD radius smaller than 32 Å, and a non-adiabatic is needed for larger radii. For the cylindrical QD both excitonic and biexcitonic complexes are considered by a configurational interaction method and for QD height of 2.3nm and parabolic confinement $\hbar\omega_e = 0.065\text{eV}$ and $\omega_e/\omega_h = 3$ the model predicts an adiabatic treatment is appropriate for describing optical transitions.

In Sec. 3.2 the Fermi Golden Rule and cumulant expansion method are used within a non-adiabatic treatment to spherical GaAs/AlAs QDs to obtain the absorption coefficient. In accordance with the experiment, we obtain: i) Large Huang-Rhys factors by two orders of magnitude than the bulk value with increasing values for smaller radii; ii) Accompanying resonances to the LO phonon satellites; iii) Red shift of the LO phonon lines and increased intensities of the accompanying resonances with temperature.

In Sec. 3.3 the Fermi Golden Rule and cumulant expansion method are used to describe the emission from the exciton and biexciton complexes of the cylindrical InAs/AlAs QDs. The presence of LO phonon replicas and emission from the excited states is explained as consequence of large Huang-Rhys factors. One finds, in accordance with the experiment, that the biexciton binding energy has a binding character (positive value), which diminishes with decreasing the radius of QD, and becomes antibinding (negative value) for flat QDs.

In conclusion, the present study emphasizes that the LO phonon coupling in the polar semiconductor QDs is an essential factor in understanding at a higher level of accuracy the optical transitions. The accordance between our results and experimental results show that the approaches we used, the Fermi Golden Rule and cumulant expansion method are useful tools in describing optical properties of semiconductor QDs. By the prediction of the Huang-Rhys factors and of the optical spectra shape, the present work is useful to people working in the field of semiconductor QDs optics, both theoreticians, in comparing different models, and experimentalists, in comparing theory and experiment.

5. Acknowledgements

The work was supported by the strategic grant POSDRU/89/1.5/S/58852, Project “Postdoctoral program for training scientific researcher” co-financed by the European Social Found within the Sectorial Operational Program Human Resources Development 2007-2013.

6. References

- Axt V. M.; Kuhn T., Vagov A., & Peeters F. M. (September 2005). Phonon-induced pure dephasing in exciton-biexciton quantum dot systems driven by ultrafast laser pulse sequences, *Physical Review B*, Vol.72, No.12, pp. 125309-1-5, ISSN 1098-0121
- Banyai, L. & Koch, S. W. (1993). *Semiconductor Quantum Dots*, World Scientific, ISBN 981-02-1390-5, Singapore
- Barker B. I.; Rayborn G. H., Ioup J. W., & Ioup G. E. (November 1991). Approximating the finite square well with an infinite well: Energies and eigenfunctions, *American Journal of Physics*, Vol.59, No.11, pp. 1038-1042, ISSN 0295-5075
- Bayer M.; Gutbrod T., Forchel A., Kulakovskii V. D., Gorbunov A., Michel M., Steffen R., & Wang K. H., Exciton complexes in $\text{In}_x\text{Ga}_{1-x}\text{As}/\text{GaAs}$ quantum dots (August 1998). *Physical Review B*, Vol.58, No.8, pp. 4740-4753, ISSN 1098-0121
- Besombes L.; Kheng K., Marsal L., & Mariette H. (March 2001). Acoustic phonon broadening mechanism in single quantum dot emission, *Physical Review B*, Vol.63, No.15, pp. 155307-1-5, ISSN 1098-0121
- Born M. & Huang K. (1998). *Dynamical Theory of Crystal Lattices*, Clarendon, ISBN 0198503695, Oxford
- Born, M. & Oppenheimer, M. (1927). Zur Quantentheorie der Molekeln. *Annalen der Physik*, Vol. 389, No. 20, pp. 457-484, ISSN 1521-3889
- Chamberlain M. P.; Trallero-Giner C. & Cardona M. (January 1995). *Physical Review B*, Vol.51, No.3, pp. 1680-1693, ISSN 1098-0121
- Chauvin N.; Salem B., Bremond G., Guillot G., Bru-Chevallier C., & Gendry. M (October 2006). Size and shape effects on excitons and biexcitons in single InAs/InP quantum dots, *Journal of Applied Physics*, Vol.100, No.7, pp. 073702-1-5, ISSN 0021-8979
- Cheche T. O; Chang M. C., Lin S. H. (March 2005). Electron-phonon interaction in absorption and photoluminescence spectra of quantum dots, *Chemical Physics*, Vol.309, No.2-3, pp. 109-114, ISSN 0301-0104
- Cheche T. O. & Chang M. C. (March 2005). Optical spectra of quantum dots: A non-adiabatic approach, *Chemical Physics Letters*, Vol. 406, pp. 479-482, ISSN 0009-2614
- Cheche T. O. (June 2009). Phonon influence on emission spectra of biexciton and exciton complexes in semiconductor quantum dots, *EPL*, Vol.86, No.6, pp. 67011-1-6, ISSN 0295-5075
- Cheche T. O., Barna E., Stamatini I. (to be published in *Physica B*)
- Dawson P.; Göbel E. O., & Pierz K. (July 2005). *Journal of Applied Physics*, Vol. 98, No.1, pp. 013541-1-4, ISSN 0021-8979

- Fomin V. M.; Gladilin V. N., Devreese J. T., Pokatilov E. P., Balaban S. N., & Klimin S. N. (January 1998). Photoluminescence of spherical quantum dots, *Physical Review B*, Vol.57, No.4, pp. 2415-2425, ISSN 1098-0121
- Fuchs R. & Kliever K.L. (December 1965). Optical Modes of Vibration in an Ionic Crystal Slab, *Physical Review*, Vol.140, No.6A, pp. A2076–A2088, ISSN 1943-2879
- García-Cristóbal A.; A. W. E. Minnaert A. W. E., V. M. Fomin V. M., J. T. Devreese J. T., A. Yu. Silov A. Yu., J. E. M. Haverkort J. E. M. , & J. H. Wolter J. H. (September 1999). Electronic Structure and Phonon-Assisted Luminescence in Self-Assembled Quantum Dots, *Physica Status Solidi (b)*, Vol.215, No.1, pp. 331-336, ISSN 0370-1972
- Grosso G. & P. Parravicini G. P. (2000). *Solid State Physics*, Academic Press, ISBN 0-12-304460-X, San Diego, San Francisco, New York, Boston, London, Sydney, Tokio, Toronto, Chapter 4
- Grundmann M., Stier O.; & Bimberg D. (October 1995). InAs/GaAs pyramidal quantum dots: Strain distribution, optical phonons, and electronic structure, *Physical Review B*, Vol.52, No.16, pp. 11969–11981, ISSN 1098-0121
- Hanamura E. (January 1988). Very large optical nonlinearity of semiconductor microcrystallites, *Physical Review B*, Vol.37, No.3, pp. 1273–1279, ISSN 1098-0121
- Haug & Koch (1993). *Quantum theory of the optical and electronic properties of semiconductors*, World Scientific, ISBN 9812387560, Singapore
- Hawrylak P. (August 1999). Exciton artificial atoms: Engineering optical properties of quantum dots, *Physical Review B*, Vol.60, No.8, pp. 5597–5608, ISSN 1098-0121;
- Heitz R., Veit M.; Ledentsov N. N., Hoffmann A., Bimberg D., Ustinov V. M., Kop'ev P. S., & Alferov Zh. I. (October 1997). Energy relaxation by multiphonon processes in InAs/GaAs quantum dots, *Physical Review B*, Vol.56, No.16, pp. 10435–10445, ISSN 1098-0121
- Huang K. & Zhu B. F. (December 1988). Dielectric continuum model and Fröhlich interaction in superlattices, *Physical Review B*, Vol.38, No.18, pp. 13377–13386, ISSN 1098-0121
- Ikezawa M.; Nair S. V., Ren H.-W., Masumoto Y., & Ruda H., Biexciton binding energy in parabolic GaAs quantum dots (August 1998). *Physical Review B*, Vol.58, No.8, pp. 4740–4753, ISSN 1098-0121
- Jacak L.; Hawrylak P., & Wójs A. (1998). *Quantum Dots*, Springer-Verlag Berlin and Heidelberg GmbH & Co. KG, ISBN 3540636536, Berlin
- Jahn H. A. & Teller E. (July 1937). Stability of Polyatomic Molecules in Degenerate Electronic States. I. Orbital Degeneracy, *Proceedings of Royal Society A*, Vol.161, pp. 220-235, ISSN 1364-5021.
- Kamada H.; Ando H., Temmyo J., & Tamamura T. (December 1998). *Physical Review B*, Vol.58, No.24, pp. 16243–16251, ISSN 1098-0121;
- Khatsevich S.; Rich D. H., Kim E. -U., & Madhukar A. (June 2005). *Journal of Applied Physics*, Vol. 97, No.12, pp. 123520 -1-8, ISSN 0021-8979
- Klein M. C.; Hache F., Ricard D., & Flytzanis C. (December 1990). Size dependence of electron-phonon coupling in semiconductor nanospheres: The case of CdSe, *Physical Review B*, Vol.42, No.17, pp. 11123–11132, ISSN 1098-0121

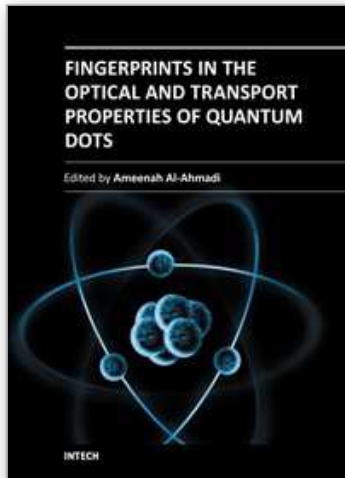
- Klimin S. N.; Pokatilov E. P., & Fomin V. M. (August 1995). Polaronic Hamiltonian and Polar Optical Vibrations in Multilayer Structures, *physica status solidi (b)*, Vol.190, No.2, pp.441-453, ISSN 0370-1972
- Mahan, G. D. (2000). *Many-Particle Physics*, Kluwer Academic/Plenum Publishers, ISBN 0-306-46338-5, New York, Boston, Dordrecht, London, Moscow, Chapter 4
- Melnikov D. V. & Fowler W. B. (December 2001). Electron-phonon interaction in a spherical quantum dot with finite potential barriers: The Fröhlich Hamiltonian, *Physical Review B*, Vol.64, No.24, pp. 245320-1-9, ISSN 1098-0121
- Menéndez E.; Trallero-Giner C. and Cardona M. (January 1997). Vibrational Resonant Raman Scattering in Spherical Quantum Dots: Exciton Effects, *Physica Status Solidi (b)*, Vol.199, No.1, pp. 81-94, ISSN 0370-1972
- Merzbacher E. (1988). *Quantum Mechanics*, J. Wiley & Sons, ISBN 0-471-88702-1, USA
- Miska P.; Paranthoen C., Even J., Bertru N., Le Corre A. & Dehaese O. (November 2002). *Journal of Physics: Condensed Matter*, Vol.14, No.47, pp. 12301, ISSN 0953-8984
- Mittin V. V.; Kochelap V. A., & Strosio M. A. (1999). *Quantum Heterostructures. Microelectronics and Optoelectronics*, Cambridge University Press, ISBN 0-521-63177-7, USA
- Mori N. & Ando T. (September 1989). Electron-optical-phonon interaction in single and double heterostructures, *Physical Review B*, Vol.40, No.9, pp. 6175-6188, ISSN 1098-0121
- Newton, M. D. & Sutin N. (1984). Electron Transfer Reactions in Condensed Phases. *Annual Reviews Physical Chemistry*, Vol. 35 (October 1984), pp. 437-480, ISSN 0066426X
- Nomura S. & Kobayashi T. (January 1992). Exciton-LO-phonon couplings in spherical semiconductor microcrystallites, *Physical Review B*, Vol.45, No.3, pp. 1305-1316, ISSN 1098-0121
- Odnoblyudov M. A.; Yassievich I. N., & Chao K. A. (December 1999). Polaron Effects in Quantum Dots, *Physical Review Letters*, Vol.83, No.23, pp. 4884-4887, ISSN 0031-9007
- Offermans P.; Koenraad P. M., Wolter J. H., Pierz K., Roy M., & Maksym P. A. (October 2005). Atomic-scale structure and photoluminescence of InAs quantum dots in GaAs and AlAs, *Physical Review B*, Vol.72, No.16, pp. 165332-1-6, ISSN 1098-0121
- Paillard M.; Marie X., Renucci P., Amand T., Jbeli A., & Gérard J. M. (February 2001). Spin Relaxation Quenching in Semiconductor Quantum Dots, *Physical Review Letters*, Vol.86, No.8, pp. 1634-1637, ISSN 0031-9007
- Peter E.; Hours J., Senellart P., Vasanelli A., Cavanna A., Bloch J., & Gérard J. M. (January 2004). Phonon sidebands in exciton and biexciton emission from single GaAs quantum dots, *Physical Review B*, Vol.69, No.4, pp. 041307(R)-1-4, ISSN 1098-0121
- Ridley B. K. (March 1989). Electron scattering by confined LO polar phonons in a quantum well, *Physical Review B*, Vol.39, No.8, pp. 5282-5286, ISSN 1098-0121
- Ridley, B. K. (1988). *Quantum Processes in Semiconductors*, Clarendon Press, ISBN 019851171X, Oxford

- Roca E.; Trallero-Giner C., & Cardona M. (May 1994). Polar optical vibrational modes in quantum dots, *Physical Review B*, Vol.49, No.19, pp. 13704–13711, ISSN 1098-0121
- Rodt S.; Schliwa A., Pötschke K., Guffarth F., & Bimberg D. (April 2005), Correlation of structural and few-particle properties of self-organized InAs/GaAs quantum dots, *Physical Review B*, Vol.71, No.15, pp. 155325-1-7, ISSN 1098-0121
- Rücker H.; Molinari E., & Lugli P. (August 1991). Electron-phonon interaction in quasi-two-dimensional systems, *Physical Review B*, Vol.44, No.7, pp. 3463–3466, ISSN 1098-0121
- Sarkar D.; van der Meulen H. P., Calleja J. M., Becker J. M., Haug R. J., & K. Pierz K. (July 2006). *Journal of Applied Physics*, Vol. 100, No.2, pp. 023109-1-4, ISSN 0021-8979
- Sarkar D.; van der Meulen H. P., Calleja J. M., Becker J. M., Haug R. J., & K. Pierz K. (February 2005). *Physical Review B*, Vol.71, No.8, pp. 081302(R)-1-4, ISSN 1098-0121
- Sénès M.; Urbaszek B., Marie X., T., Tribollet J., Bernardot F., Testelin C., Chamarro M., & Gérard J.-M. (March 2005). *Physical Review B*, Vol.71, No.11, pp. 115334-1-6, ISSN 1098-0121
- Sercel P. C. & Vahala K. J. (August 1990). Analytical formalism for determining quantum-wire and quantum-dot band structure in the multiband envelope-function approximation, *Physical Review B*, Vol.42, No.6, pp. 3690–3710, ISSN 1098-0121
- Shumway J.; Franceschetti A., & Zunger A. (March 2001). Correlation versus mean-field contributions to excitons, multiexcitons, and charging energies in semiconductor quantum dots, *Physical Review B*, Vol.63, No.8, pp. 155316-1-13, ISSN 1098-0121
- Stier O.; Schliwa A., Heitz R., Grundmann M., & Bimberg D. (March 2001). Stability of Biexcitons in Pyramidal InAs/GaAs Quantum Dots, *physica status solidi (b)*, Vol.215, No.1, pp.115-118, ISSN 0370-1972
- Takagahara T. (February 1993). Effects of dielectric confinement and electron-hole exchange interaction on exciton states in semiconductor quantum dots, *Physical Review B*, Vol.47, No.8, pp. 4569–4584, ISSN 1098-0121
- Takagahara T. (July 1999). Theory of exciton dephasing in semiconductor quantum dots, *Physical Review B*, Vol.60, No.4, pp. 2638–2652, ISSN 1098-0121
- Vasilevskiy M. I.; Anda E. V., & Makle S.S. (July 2004). Electron-phonon interaction effects in semiconductor quantum dots: A nonperturbative approach, *Physical Review B*, Vol.72, No.12, pp. 125309-1-5, ISSN 1098-0121
- Verzelen O.; Ferreira R., & Bastard G. (April 2002). Exciton Polarons in Semiconductor Quantum Dots, *Physical Review Letters*, Vol.88, No.14, pp. 146803-1-4, ISSN 0031-9007
- Voigt J.; Spiegelberg F., & Senoner M., Band parameters of CdS and CdSe single crystals determined from optical exciton spectra (January, 1979). *Physica Status Solidi (b)*, Vol.91, No.1, pp. 189-199, ISSN 0370-1972

- Vurgaftman I.; Meyer J. R., & Ram-Mohan L. R. (February 2001). Band parameters for III-V compound semiconductors and their alloys, *Journal of Applied Physics*, Vol.89, No.11, pp. 5815- 5875, ISSN 0021-8979
- Woggon, U. (1997), *Optical Properties of Semiconductor Quantum Dots*, Springer, ISBN 3540609067, Berlin, Chapter 5
- Zutić I.; Fabian J., & S. Das Sarma D. (2004), *Review of Modern Physics*, Vol.76, No.2, pp. 323-410, ISSN 0034-6861

IntechOpen

IntechOpen



Fingerprints in the Optical and Transport Properties of Quantum Dots

Edited by Dr. Ameenah Al-Ahmadi

ISBN 978-953-51-0648-7

Hard cover, 468 pages

Publisher InTech

Published online 13, June, 2012

Published in print edition June, 2012

The book "Fingerprints in the optical and transport properties of quantum dots" provides novel and efficient methods for the calculation and investigating of the optical and transport properties of quantum dot systems. This book is divided into two sections. In section 1 includes ten chapters where novel optical properties are discussed. In section 2 involve eight chapters that investigate and model the most important effects of transport and electronics properties of quantum dot systems This is a collaborative book sharing and providing fundamental research such as the one conducted in Physics, Chemistry, Material Science, with a base text that could serve as a reference in research by presenting up-to-date research work on the field of quantum dot systems.

How to reference

In order to correctly reference this scholarly work, feel free to copy and paste the following:

Cheche Tiberius and Emil Barna (2012). Influence of Optical Phonons on Optical Transitions in Semiconductor Quantum Dots, Fingerprints in the Optical and Transport Properties of Quantum Dots, Dr. Ameenah Al-Ahmadi (Ed.), ISBN: 978-953-51-0648-7, InTech, Available from: <http://www.intechopen.com/books/fingerprints-in-the-optical-and-transport-properties-of-quantum-dots/influence-of-optical-phonons-on-optical-transitions-in-semiconductor-quantum-dots>

INTECH
open science | open minds

InTech Europe

University Campus STeP Ri
Slavka Krautzeka 83/A
51000 Rijeka, Croatia
Phone: +385 (51) 770 447
Fax: +385 (51) 686 166
www.intechopen.com

InTech China

Unit 405, Office Block, Hotel Equatorial Shanghai
No.65, Yan An Road (West), Shanghai, 200040, China
中国上海市延安西路65号上海国际贵都大饭店办公楼405单元
Phone: +86-21-62489820
Fax: +86-21-62489821

© 2012 The Author(s). Licensee IntechOpen. This is an open access article distributed under the terms of the [Creative Commons Attribution 3.0 License](#), which permits unrestricted use, distribution, and reproduction in any medium, provided the original work is properly cited.

IntechOpen

IntechOpen